Published OnlineFirst September 9, 2011; DOI:10.1158/1078-0432.CCR-11-0313

showed higher promoter activity than other deletion mutants. In transient-cotransfection assays, simultaneous expression of Miz-1 increased the luciferase activities driven by the *NLRR3* promoter (−677 to +67; Fig. 3B, left).

On the contrary, overexpression of MYCN resulted in reduced activity of the *NLRR3* promoter (Supplementary Fig. S4B). These results suggest that Miz-1 and MYCN together contribute to the transcriptional regulation of the *NLRR3* gene. Indeed, the activation of the *NLRR3* promoter by exogenous Miz-1 expression in SH-SY5Y cells was suppressed by coexpression of MYCN in a dose-dependent manner (Fig. 3B, right). The luciferase activities driven by the core promoter region (−35 to +67) also showed a similar result (data not shown). It was reported that a transcriptional suppression of the MYCN-targeted genes occurs when MYCN forms a complex with Miz-1 and Max (19). To make certain of the physical interaction between MYCN and Miz-1, the whole cell lysates prepared from the SK-N-AS cells cotransfected with *MYCN* and *Miz-1* were subjected to an immunoprecipitation assay. As shown in Fig. 3C, coimmunoprecipitation using either MYCN or Miz-1 antibody confirmed that MYCN and Miz-1 formed a complex in SK-N-AS cells as previously reported in non-NBL cell lines (38). Moreover, ChIP analysis revealed that MYCN, Max, and Miz-1 were recruited onto the same promoter region of *NLRR3* (−164 to +67) in SH-SY5Y cells (Fig. 3D). Hence, MYCN negatively regulates *NLRR3* expression by forming a transcriptional complex with Miz-1 in NBL cells.

Increased expression of *NLRR3* and *Miz-1* in favorable neuroblastoma

In our previous report, *NLRR3* is highly expressed in favorable NBLs with a single copy of *MYCN* as compared with NBLs with *MYCN* amplification. To evaluate whether the expression pattern of *Miz-1*, *NLRR3*, and *MYCN* observed in NBL cell lines is consistent in primary NBLs, we analyzed expression levels of those 3 genes in 16 favorable (stages 1 or 2, high expression of *TrkA* and a single copy of *MYCN*) and 16 unfavorable (stages 3 or 4, low expression of TrkA and amplification of *MYCN*) NBL samples by semiquantitative RT-PCR. As shown in Supplementary Fig. S5A, *NLRR3* and *Miz-1* were expressed at higher levels in favorable NBLs than those in unfavorable tumors, whereas the levels of *MYCN* expression were predominantly high in the unfavorable tumors. The expression levels of *NLRR3* and *Miz-1* were also higher in the cell lines with a single copy of *MYCN* than those with *MYCN* amplification, indicating evidence of a positive correlation between *NLRR3* and *Miz-1* expressions and of an inverse correlation between *NLRR3* and *MYCN* expressions (Supplementary Fig. S5B). Those expression patterns were further assessed by immunohistochemistry for NLRR3, MYCN, and Miz-1 in primary NBL tissues (Supplementary Fig. S5C). We carried out immunohistochemical staining on all 11 available paraffin-embedded primary NBL tissues, including 5 NBLs with a single copy of *MYCN* and favorable histology according to INPC (39), 3 NBLs carrying a single copy of *MYCN* with unfavorable histology, and 3 NBLs with *MYCN* amplification and unfavorable histology. As shown in Supplementary Fig. S5C and Supplementary Table S1, the absence of MYCN amplification was associated with strong positive staining of NLRR3 and Miz-1 in all examined samples except one (case 8). All 3 NBLs with *MYCN* amplification showed weak staining for both NLRR3 and Miz-1.

Low expression of *NLRR3* and *Miz-1* is associated with an unfavorable outcome of neuroblastoma

To evaluate whether a statistically significant relationship exists between the patients' survival periods and the expression of *NLRR3*, *Miz-1*, or *MYCN* in primary NBLs, we quantitatively measured the expression levels of *NLRR3*, *Miz-1*, and *MYCN* mRNAs in 87 primary NBLs by using the quantitative real-time PCR method. The clinical features of each NBL samples are listed in Supplementary Table S2. As shown in Table 1, high levels of *NLRR3* expression were significantly associated with younger age ($P = 0.047$), single copy of *MYCN* ($P = 0.047$), favorable disease stages ($P = 0.041$), high levels of *TrkA* expression ($P = 0.042$), and diploid DNA index ($P = 0.003$), but not with tumor origin ($P = 0.933$). A high level of *Miz-1* expression was also significantly associated with younger age ($P = 0.004$), single copy of *MYCN* ($P = 0.004$), favorable disease stages ($P = 0.001$), and high levels of *TrkA* expression ($P = 0.001$), but not with DNA index ($P = 0.060$) and tumor origin ($P = 0.959$). In contrast, a high level of *MYCN* expression was significantly associated with *MYCN* amplification ($P = 0.0001$), advanced disease stages ($P = 0.0031$), low levels of *TrkA* expression ($P = 0.026$), and tumor origin ($P = 0.028$), but not with DNA index ($P = 0.079$), which is consistent with the previous reports (23, 40, 41). There was also a marginal association with patient age ($P = 0.063$). These results suggest that high expression of *NLRR3* and *Miz-1* is well associated with conventional prognostic markers predicting a favorable NBL outcome.

To examine whether the expression levels of *NLRR3*, *Miz-1* and/or *MYCN* have a prognostic significance in primary NBLs, we employed log-rank tests for gene-expression data (Supplementary Table S3). There were significant differences in survival rates in the groups of patients with high and low expression of *NLRR3*, *Miz-1*, and *MYCN*. Patients with high expression of *NLRR3* or *Miz-1* had a higher survival rate than patients with low expression of *NLRR3* or *Miz-1*, and such a difference in survival rate was statistically significant ($P = 0.0023$ and $P = 0.00060$, respectively). However, a patient with high *MYCN* expression was associated with a lower survival rate than that of the *MYCN* low subset ($P < 0.00001$; Supplementary Table S3). Figure 4 shows Kaplan–Meier cumulative survival curves for 87 patients with NBL in terms of expression of *NLRR3*, *Miz-1* and *MYCN*. High expression of *NLRR3* and that of *Miz-1* were significantly associated with good survival ($P = 0.0023$ and $P = 0.00060$, respectively; Fig. 4A, left and right). As already known, high expression of *MYCN*

Published OnlineFirst September 9, 2011; DOI:10.1158/1078-0432.CCR-11-0313

Table 1. Correlation between expression of *NLRR3* or *MYCN* or *Miz-1* and other prognostic factors (Student *t* test)

		NLRR3		*MYCN*		*Miz-1*	
Variable	**No.**	**Mean ± SEM**	***P***	**Mean ± SEM**	***P***	**Mean ± SEM**	***P***
Age, y							
<1	32	0.043 ± 0.011	0.047[a]	0.034 ± 0.013	0.063	0.091 ± 0.019	0.004[a]
≥1	55	0.024 ± 0.003		0.141 ± 0.043		0.042 ± 0.007	
MYCN copy number							
Single copy	58	0.041 ± 0.006	0.047[a]	0.022 ± 0.016	0.0001[a]	0.077 ± 0.012	0.004[a]
Amplified	29	0.019 ± 0.004		0.222 ± 0.053		0.026 ± 0.004	
Tumor stage							
1, 2, 4s	34	0.043 ± 0.009	0.041[a]	0.007 ± 0.002	0.0031[a]	0.093 ± 0.017	0.001[a]
3, 4	53	0.024 ± 0.003		0.144 ± 0.036		0.039 ± 0.007	
TrkA expression							
High	24	0.047 ± 0.013	0.042[a]	0.009 ± 0.003	0.026[a]	0.104 ± 0.024	0.001[a]
Low	61	0.025 ± 0.004		0.125 ± 0.032		0.044 ± 0.006	
DNA index							
Diploidy	42	0.019 ± 0.003	0.003[a]	0.121 ± 0.037	0.079	0.049 ± 0.008	0.06
Aneuploidy	31	0.050 ± 0.010		0.034 ± 0.023		0.085 ± 0.019	
Tumor origin							
Adrenal gland	48	0.032 ± 0.007	0.933	0.135 ± 0.035	0.028[a]	0.059 ± 0.012	0.959
Others	39	0.032 ± 0.004		0.034 ± 0.025		0.060 ± 0.011	

[a]$P < 0.05$.

was strongly associated with a poor prognosis of NBL ($P < 0.00001$; Fig. 4A, middle). Remarkably, the combination of low levels of both *NLRR3* and *Miz-1* expressions showed a significantly worse prognosis as compared with the other combination, high *NLRR3* and *Miz-1* expressions ($P = 0.0012$; Fig. 4C). Furthermore, the combination of low expression of *NLRR3* and high expression of *MYCN* showed a significantly worse prognosis than the combination of high expression of *NLRR3* and low expression of *MYCN* ($P < 0.00001$; Fig. 4B). In NBLs with low expression of *MYCN*, the expression levels of *NLRR3* could segregate the prognosis into good and intermediate groups.

The univariate Cox regression analysis shown in Table 2 was employed to examine the individual relationship of each variable to survival. The results in Table 2 showed that *NLRR3* expression, *MYCN* expression, *Miz-1* expression, age, *MYCN* amplification, stage *TrkA* expression, and origin were of prognostic importance, supporting the results of the log-rank test. Moreover, the multivariate Cox models were fitted to assess the predictive importance of NLRR3 expression for survival after controlling other prognostic factors. The results in Table 2 showed that *NLRR3* expression was significantly associated with survival after controlling *TrkA* expression ($P = 0.0212$), suggesting that *NLRR3* expression was an independent prognostic factor from *TrkA* expression (Table 2). This suggests that *NLRR3* expression is associated with survival after controlling *MYCN* expression ($P = 0.0610$), *Miz-1* expression ($P = 0.1510$), *MYCN* amplification ($P = 0.1210$), and stage ($P = 0.1040$), and also supports that *NLRR3* expression could serve as a prognostic biomarker for NBL tumors dependent on both MYCN and Miz-1 expression as well as *MYCN* amplification.

Discussion

In primary human NBLs, *MYCN* is frequently amplified and thereby one of the most important prognostic factors. In this study, we found that *NLRR3* is a direct target of MYCN but its expression is negatively regulated by MYCN in association with Miz-1. In primary NBLs, both *NLRR3* and *Miz-1* are expressed at significantly high levels in favorable NBLs and downregulated in *MYCN*-amplified aggressive tumors.

In general, favorable NBL cells show more differentiated features than unfavorable cells (30). The treatment of NBL cells with ATRA induces neuronal differentiation accompanied with growth inhibition and reduction of *MYCN* expression (33). Under such conditions, *NLRR3* is induced while *MYCN* is decreased (Figs. 1 and 2). These results suggest a functional inverse relationship between MYCN and NLRR3 in cellular differentiation and tumor development. In some NBL cell lines, siRNA-mediated knockdown of endogenous MYCN caused NLRR3 induction; conversely, ectopic expression of MYCN resulted in a decreased expression of *NLRR3*. Hence, the inverse regulatory relationship between NLRR3 and MYCN may be present as a

Published OnlineFirst September 9, 2011; DOI:10.1158/1078-0432.CCR-11-0313

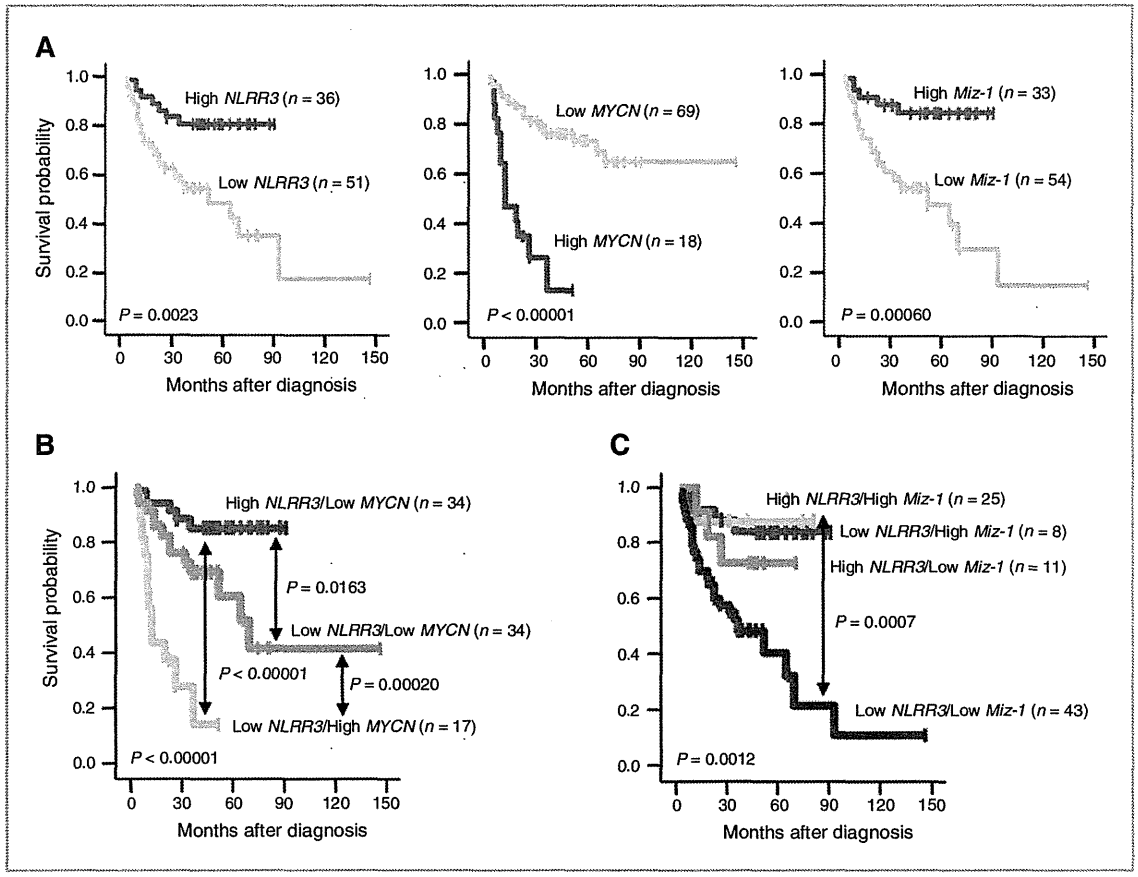

Figure 4. Real-time PCR analysis for the expression of *NLRR3*, *MYCN*, and *Miz-1* in 87 primary NBLs. Kaplan–Meier survival curves of patients with NBLs on the basis of higher or lower expression levels of *NLRR3* (A, left); *MYCN* (A, middle); *Miz-1* (A, right); *NLRR3* and *MYCN* (B); or *NLRR3* and *Miz-1* (C). In case of *NLRR3* and *MYCN* survival curve, high NLRR3/high MYCN group was excluded because this group consists of only 2 samples. Relative expression levels of *NLRR3* or *MYCN* or *Miz-1* mRNA were determined by calculating the ratio between *GAPDH* and *NLRR3* or *MYCN* or *Miz-1*.

consequence of MYCN-induced transcriptional downregulation of *NLRR3*.

MYCN protein is an important regulator of many cellular processes, including growth, proliferation, differentiation, and apoptosis (42). A part of these diverse cellular functions of MYCN may be due to the combined abilities of both activating and repressing transcription of the target genes (42). Transcriptional activation by MYCN occurs *via* dimerization with its partner protein, Max, and direct binding to specific DNA sequences named E-boxes. MYCN directly binds and stimulates the expression of approximately 4,000 of the E-box containing genes (43). Although heterodimerization of Max with MYCN is necessary to regulate gene expression, the other proteins including *Miz-1* may bind to C-terminal MYCN in addition to Max (19, 20, 44). Concurrent binding of these factors redirects the MYCN/Max dimer to noncanonical sites such as the initiator element, where this complex might prevent the efficient binding of basal transcriptional machinery or coactivators necessary for transactivation, resulting in repression of gene expression (38, 44). The dimerization with MYCN switches Miz-1 from a transcriptional activator to a repressor of the target genes, likely by preventing the interaction of Miz-1 with its own coactivator (19, 20). Several studies have shown that Miz-1 binds and activates the promoter of several genes, including $p15^{INK4b}$ and $p21^{CIP1}$, and the transactivation can be negatively regulated by its association with MYCN (16, 17, 29). Regarding the reduction of NLRR3 expression observed in this study, Miz-1 seems to be a key molecule forming a transcription factor complex with MYCN. Because Miz-1 itself acts as an activator of *NLRR3* promoter, *NLRR3* expression may be switched on and off through Miz-1 in the absence and presence of MYCN, respectively. Although the expression levels of Miz-1 in unfavorable NBLs are relatively low, its amount still may be enough to act with MYCN to inhibit transactivation of *NLRR3* in NBLs.

Published OnlineFirst September 9, 2011; DOI:10.1158/1078-0432.CCR-11-0313

Table 2. Multiple Cox regression model using NLRR3 expression and dichotomous factors of MYCN expression, Miz-1 expression, age, MYCN amplification, stage, TrkA expression, and origin ($n = 87$)

Model	Factor	*P*	HR (95% CI)
Univariate analysis			
A	*NLRR3* mRNA expression (high vs. low)	0.0041[a]	0.291 (0.125–0.678)
B	*MYCN mRNA* expression (high vs. low)	<0.0001[a]	5.050 (2.450–10.40)
C	*Miz-1* mRNA expression (high vs. low)	0.0021[a]	0.212 (0.080–0.561)
D	Age (≥1 vs. <1 y)	0.0161[a]	0.309 (0.119–0.803)
E	*MYCN* amplification (single copy vs. amplified)	<0.0001[a]	4.628 (2.281–9.387)
F	Stage (1,2,4s vs. 3,4)	0.0010[a]	12.66 (3.023–53.09)
G	*TrkA* expression (high vs. low)	0.0070[a]	7.180 (1.714–30.07)
H	Origin (adrenal gland vs. others)	0.0480[a]	2.125 (1.005–4.491)
Multivariate analysis			
A	*NLRR3* mRNA expression (high vs. low)	0.061	0.424 (0.172–1.041)
	MYCN mRNA expression (high vs. low)	0.0011[a]	3.707 (1.735–7.921)
B	*NLRR3* mRNA expression (high vs. low)	0.151	0.503 (0.198–1.283)
	Miz-1 mRNA expression (high vs. low)	0.0301[a]	0.304 (0.104–0.893)
C	*NLRR3* mRNA expression (high vs. low)	0.0150[a]	0.347 (0.148–0.814)
	Age (≥1 vs. <1 y)	0.053	0.384 (0.146–1.013)
D	*NLRR3* mRNA expression (high vs. low)	0.121	0.545 (0.253–1.173)
	MYCN amplification (single copy vs. amplified)	0.0001[a]	3.940 (1.893–8.203)
E	*NLRR3* mRNA expression (high vs. low)	0.104	0.493 (0.210–1.156)
	Stage (1, 2, 4s vs: 3, 4)	0.0020[a]	10.108 (2.359–43.309)
F	*NLRR3* mRNA expression (high vs. low)	0.0212[a]	0.361 (0.152–0.863)
	TrkA expression (high vs. low)	0.0163[a]	5.892 (1.395–24.901)
G	*NLRR3* mRNA expression (high vs. low)	0.0070[a]	0.308 (0.132–0.720)
	Origin (adrenal gland vs. others)	0.084	1.937 (0.914–4.104)

NOTE: All variables with 2 categories. HR shows the relative risk of death of first category relative to the second.
[a]$P < 0.05$.

Inhibition of cellular differentiation is one of the well-known biological functions of MYCN. Because differentiated NBL cells have a high expression of NLRR3 instead of MYCN, the reduced expression of NLRR3 in undifferentiated, unfavorable NBL cells may propose an important component of the mechanism by which MYCN functions against cell differentiation. As ectopic expression of NLRR3 induced morphologic changes indicative of neuronal differentiation accompanying with neurite outgrowth (data not shown), the downregulation of NLRR3 by MYCN might contribute to the well-documented stimulation of cell proliferation by MYCN. Although there are MYCN target genes that are potentially involved in cell-cycle progression, including *α-prothymosin, ornithine decarboxylase, MCM7, ID2, MDM2,* and *NLRR1* (27, 36, 45–47), suppression of NLRR3 might have an additive effect on NBL cell proliferation. Our log-rank test showed that expression of NLRR3 is well associated with a favorable prognosis, suggesting its involvement in NBL differentiation. Of more interest, NLRR3 and NLRR1 seem to function oppositely in NBL. Thus, the expression of NLRR3 is a new prognostic indicator of NBL and may be involved in regulating the biology of the tumor.

Collectively, our present findings suggest that the repression of NLRR3 mediated by MYCN requires an association with Miz-1 and also contributes to the favorable outcome of NBLs. The expression pattern of NLRR3, Miz-1, and MYCN might play an important role in defining the clinical behavior of NBLs. Because NLRR3 is an orphan receptor, the future discovery of its ligand(s) may unveil the molecular mechanism of tumorigenesis, differentiation, and proliferation of NBL. Further investigation is necessary to clarify whether NLRR3 is an important primary cue for developing novel diagnostic and therapeutic strategies against high-risk NBLs.

Disclosure of Potential Conflicts of interest

No potential conflicts of interest were disclosed.

Acknowledgments

The authors thank Drs. Y. Nakamura and E. Isogai (Chiba Cancer Center Research Institute, Chiba, Japan) for their outstanding technical assistance, and Dr. Hiroki Nagase (Chiba Cancer Center Research Institute, Chiba, Japan) and Ms. Paula D. Jones (Roswell Park Cancer Institute, Buffalo, NY) for critical reading of the article.

Published OnlineFirst September 9, 2011; DOI:10.1158/1078-0432.CCR-11-0313

Grant Support

This work was supported in part by a grant-in-aid from the Ministry of Health, Labour and Welfare for Third Term Comprehensive Control Research for Cancer (A. Nakagawara), a grant-in-aid for Scientific Research on Priority Areas from the Ministry of Education, Culture, Sports, Science and Technology, Japan (A. Nakagawara), and a grant-in-aid for Scientific Research from the Japanese Society for the Promotion of Science (A. Takatori and A. Nakagawara).

The costs of publication of this article were defrayed in part by the payment of page charges. This article must therefore be hereby marked *advertisement* in accordance with 18 U.S.C. Section 1734 solely to indicate this fact.

Received February 3, 2011; revised August 3, 2011; accepted August 9, 2011; published OnlineFirst September 9, 2011.

References

1. Westemann F, Schwab M. Genetic parameters of neuroblastomas. Cancer Lett 2002;184:127–47.
2. Brodeur GM, Nakagawara A. Molecular basis of clinical heterogeneity in neuroblastoma. Am J Pediatr Hematol Oncol 1992;14: 111–6.
3. Nakagawara A, Arima M, Azar CG, Scavarda NJ, Brodeur GM. Inverse relationship between trk expression and N-myc amplification in human neuroblastomas. Cancer Res 1992;52:1364–68.
4. Nakagawara A, Arima-Nakagwara M, Scavarda NJ, Azar CG, Cantor AB, Brodeur GM. Association between high levels of expression of the TRK gene and favorable outcome in human neuroblastoma. New Engl J Med 1993;328:847–54.
5. Nakagawara A, Azar CG, Scavarda NJ, Brodeur GM. Expression and function of TRK-B and BDNF in human neuroblastomas. Mol Cell Biol 1994;14:759–67.
6. Nakagawara A, Arima-Nakagawara M, Azar CG, Scavarda NJ, Brodeur GM. Clinical significance of expression of neurotrophic factors and their receptors in neuroblastoma. Prog Clin Biol Res 1994;385: 155–61.
7. Seeger RC, Brodeur GM, Sather H, Dalton A, Siegel SE, Wong KY, et al. Associations of multiple copies of the N-myc oncogene with rapid progression of neuroblastomas. New Engl J Med 1985;313: 1111–6.
8. Kohl NE, Gee CE, Alt FW. Activated expression of the N-myc gene in human neuroblastomas and related tumors. Science 1984;226: 1335–7.
9. Nisen PD, Waber PG, Rich MA, Pierce S, Garvin JR, Gilbert F, et al. N-myc oncogene RNA expression in neuroblastoma. J Natl Cancer Inst 1988;80:1633–7.
10. Slavc I, Ellenbogen R, Jung WH, Vawter GF, Kretschmar C, Grier H, et al. Myc gene amplification and expression in primary human neuroblastoma. Cancer Res 1990;50:1459–63.
11. Seeger RC, Wada R, Brodeur GM, Moss TJ, Bjork RL, Sousa L, et al. Expression of N-myc by neuroblastomas with one or multiple copies of the oncogene. Prog Clin Biol Res 1988;271:41–9.
12. Schwab M, Ellison J, Busch M, Rosenau W, Varmus HE, Bishop JM. Enhanced expression of the human gene N-myc consequent to amplification of DNA may contribute to malignant progression of neuroblastoma. Proc Natl Acad Sci U S A 1984;81:4940–4.
13. Cohn SL, Tweddle DA. MYCN amplification remains prognostically strong 20 years after its "clinical debut". Eur J Cancer 2004;40: 2639–42.
14. Strieder V, Lutz W. Regulation of N-myc expression in development and diseases. Cancer Lett 2002;180:107–19.
15. Kouzarides T, Ziff E. The role of the leucine zipper in the fos-jun interaction. Nature 1988;336:646–51.
16. Landschulz WH, Johnson PF, Mcknight SL. The leucine zipper: a hypothetical structure common to a new class of DNA binding proteins. Science 1988;240:1759–64.
17. Alex R, Sozeri O, Meyer S, Dildrop R. Determination of the DNA sequence recognized by the bHLH-zip domain of the N-Myc protein. Nucleic Acids Res 1992;20:2257–63.
18. Blackwood EM, Kretzner L, Eisenman RN. Myc and Max function as a nucleoprotein complex. Curr Opin Genet Dev 1992;2:227–35.
19. Staller P, Peukert K, Kiermaier A, Seoane J, Lukas J, Karsunky H, et al. Repression of p15INK4b expression by Myc through association with Miz-1. Nature Cell Biol 2001;3:392–9.
20. Wu S, Cetinkaya C, Munoz-Alonso MJ, Von der Lehr N, Bahram F, Beuger V, et al. Myc represses differentiation-induced p21CIP1 expression via Miz-1-dependent interaction with the p21 core promoter. Oncogene 2003;22:351–60.
21. Zhang J, Li F, Liu X, Shen L, Liu J, Su J, et al. The repression of human differentiated-related gene NDRG2 expression by Myc via Miz-1 dependent interaction with the NDRG2 core promoter. J Biol Chem 2006;281:39159–68.
22. Koppen A, Ait-Aissa R, Hopman S, Koster J, Haneveld F, Versteeg R, et al. Dickkopf-1 is down-regulated by MYCN and inhibits neuroblastoma cell proliferation. Cancer Lett 2007;256:218–28.
23. Hamano S, Ohira M, Isogai E, Nakada K, Nakagawara A. Identification of novel human neuronal leucine-rich repeat (hNLRR) family genes and inverse association of expression of Nbla10449/hNLRR-1 and Nbla10677/hNLRR-3 with the prognosis of primary neuroblastomas. Int J Oncol 2004;24:1457–66.
24. Ohira M, Morohashi A, Inuzuka H, Shishikura T, Kawamoto T, Kageyama H, et al. Expression profiling and characterization of 4200 genes cloned from primary neuroblastomas: identification of 305 genes differentially expressed between favorable and unfavorable subsets. Oncogene 2003;22:5525–36.
25. Hayata T, Uochi T, Asashima M. Molecular cloning of XNLRR-1, a Xenopus homolog of mouse neuronal leucine-rich repeat protein expressed in the developing Xenopus nervous system. Gene 1998;221:159–66.
26. Fukamachi K, Matsuoka Y, Ohno H, Hamaguchi T, Tsuda H. Neuronal leucine-rich repeat protein-3 amplifies MAPK activation by epidermal growth factor through a carboxyl-terminal region containing endocytosis motifs. J Biol Chem 2002;277:43549–52.
27. Hossain MS, Ozaki T, Wang H, Nakagawa A, Takenobu H, Ohira M, et al. N-MYC promotes cell proliferation through a direct transactivation of neuronal leucine-rich repeat protein-1 (NLRR1) gene in neuroblastoma. Oncogene 2008;27:6075–82.
28. Ishii N, Wanaka A, Tohyama M. Increased expression of NLRR-3 mRNA after cortical brain injury in mouse. Molecular Brain Research 1996;40:148–52.
29. Brodeur GM, Pritchard J, Berthold F, Carlsen NL, Castel V, Castelberry RP, et al. Revisions of the international criteria for neuroblastoma. Diagnosis, staging, and response to treatment. J Clin Oncol 1993;11:1466–77.
30. Matsumura T, Iehara T, Sawada T, Tsuchida Y. Prospective study for establishing the optimal therapy of infantile neuroblastoma in Japan. Med Pediatr Oncol 1998;31:210.
31. Kaneko M, Nishihira H, Mugishima H, Ohnuma N, Nakada K, Kawa K, et al. Stratification of treatment of stage 4 neuroblastoma patients based on N-myc amplification status. Study Group of Japan for Treatment of Advanced Neuroblastoma, Tokyo, Japan. Med Pediatr Oncol 1998;31:1–7.
32. Melino G, Thiele CJ, Knight RA, Piacentini M. Retinoids and the control of growth/death decisions in human neuroblastoma cell lines. J Neurooncol 1997;31:65–83.
33. Thiele CJ, Reynolds CP, Israel MA. Decreased expression of N-myc precedes retinoic acid-induced morphological differentiation of human neuroblastoma. Nature 1985;313:404–6.
34. Niizuma H, Nakamura Y, Ozaki T, Nakanishi H, Ohira M, Isogai E, et al. Bcl-2 is a key regulator for the retinoic acid-induced apoptopic cell death in neuroblastoma. Oncogene 2006;25:5046–55.
35. Bjelfman C, Meyerson G, Cartwright CA, Mellstrom K, Hammerling U, Pahlman S. Early activation of endogenous pp60src kinase activity during neuronal differentiation of cultured human neuroblastoma cells. Mol Cell Biol 1990;10:361–70.

Published OnlineFirst September 9, 2011; DOI:10.1158/1078-0432.CCR-11-0313

36. Lutz W, Stohr M, Schurmann J, Wenzel A, Lohr A,Schwab M. Conditional expression of N-myc in human neuroblastoma cells increases expression of α-prothymosin and ornithine decarboxylase and accelerates progression into S-phase after mitogenic stimulation of quiescent cells. Oncogene 1996;13:803–12.
37. Chen L, Peng Z, Bateman E. In vivo interactions of the Acanthamoeba TBP gene promoter. Nucleic acids Res 2004;32: 1251–60.
38. Peukert K, Staller P, Schneider A, Carmichael G, Hanel F,Eilers M. An alternative pathway for gene regulation by Myc. EMBO J 1997;16: 5672–86.
39. Shimada H, Ambros IM, Dehner LP, Hata J, Joshi VV, Roald B, et al. The International Neuroblastoma Pathology Classification (the Shimada System). Cancer 1999;86: 364–72.
40. Ikegaki N, Gotoh T, Kung B, Riceberg JS, Kim DY, Zhao H, et al. De novo identification of MIZ-1 (ZBTB17) encoding a MYC-interacting zinc-finger protein as a new favorable neuroblastoma gene. Clin Cancer Res 2007;13:6001–9.
41. Tang XX, Zhou H, Kung B, Kim DY, Hicks SL, Cohn SL, et al. The MYCN enigma: significance of MYCN expression in neuroblastoma. Cancer Res 2006;66:2826–33.
42. Pelengaris S, Khan M, Evan G. c-MYC: more than just a matter of life and death. Nat Rev Cancer 2002;2:764–76.
43. Levens DL. Reconstructing MYC. Genes dev 2003;17:1071–7.
44. Wanzel M, Herold S, Eilers M. Transcriptional repression by Myc. Trends Cell Biol 2003;13:146–50.
45. Shohet JM, Hicks MJ, Plon SE, Burlingame SM, Stuart S, Chen SY, et al. Minichromosome maintenance protein MCM7 is a direct target of the MYCN transcription factor in neuroblastoma. Cancer Res 2002;62:1123–8.
46. Iasorella A, Noseda M, Beyna M, Yokota Y, Iavarone A. Id2 is a retinoblastoma protein target and mediates signaling by Myc oncoproteins. Nature 2000;407:592–8.
47. Slack A, Chen Z, Tonelli R, Pule M, Hunt L, Pession A, et al. The p53 regulatory gene MDM2 is a direct transcriptional target of MYCN in neuroblastoma. Proc Natl Acad Sci U S A 2005;102:731–6.

Int J Clin Oncol (2012) 17:190–195
DOI 10.1007/s10147-012-0415-7

REVIEW ARTICLE

Molecular and genetic bases of neuroblastoma

Takehiko Kamijo · Akira Nakagawara

Received: 11 April 2012 / Published online: 16 May 2012

Abstract Neuroblastoma, which is derived from the sympathetic nervous system, is the second most common pediatric solid malignant tumor. This pediatric tumor has a heterogeneous course, ranging from spontaneous regression to inexorable progression and death, depending on the biological features of the tumor. Identification of risk groups on the basis of clinical and molecular prognostic variables has allowed tailor-made therapy to improve outcomes and minimize the risk of deleterious consequences of therapy. In Japan, current therapeutic stratification of patients with neuroblastoma is based on risk assessment according to combinations of age, tumor stage, *MYCN* status, DNA ploidy status, and histopathology; however, unfavorable neuroblastoma is still one of the most difficult tumors to cure, with only 40 % long-term survival despite intensive multimodal therapy. Further refined therapeutic stratification based on newly identified prognostic factors will be required to improve the outcome of patients with unfavorable neuroblastoma and reduce the side effects of therapies for patients with favorable neuroblastoma. In the present review, we describe recent topics on the molecular and genetic bases of neuroblastoma; we hope this review will be helpful for understanding the mechanism of neuroblastoma tumorigenesis and aggressiveness and for developing a new therapeutic stratification and new protocols for neuroblastoma treatments.

Keywords Neuroblastoma · Molecular and genetic abnormality

T. Kamijo (✉)
Division of Biochemistry and Molecular Carcinogenesis,
Chiba Cancer Center Research Institute,
666-2 Nitona, Chuo-ku, Chiba, Chiba 260-8717, Japan
e-mail: tkamijo@chiba-cc.jp

A. Nakagawara (✉)
Division of Biochemistry and Innovative Cancer Therapeutics,
Chiba Cancer Center Research Institute,
666-2 Nitona, Chuo-ku, Chiba, Chiba 260-8717, Japan
e-mail: akiranak@chiba-cc.jp

Clinical and biological features of neuroblastoma

Neuroblastoma (NB) is one of the most common malignant solid tumors occurring in infancy and childhood and accounts for 10 % of all pediatric cancers [1–3]. NB is diagnosed at a median age of about 17 months and can arise anywhere along the sympathetic nervous system, with the majority of the tumors occurring in the adrenal medulla. NB tumors in the neck or upper chest can cause Horner's syndrome (ptosis, miosis, and anhidrosis). NB tumors along the spinal column can expand through the intra-foraminal spaces and cause cord compression, resulting in paralysis. Higher-stage NBs often infiltrate adjacent organs, surround critical nerves and vessels, and are largely unresectable at the time of diagnosis, although many lower-stage NBs are encapsulated and can be surgically excised. Advanced NBs typically metastasize to regional lymph nodes and to the bone marrow via the hematopoietic system. NB cells metastatic to marrow can infiltrate cortical bone. NBs can also metastasize to the liver, most notably in patients with stage 4S tumors, which occur in about 5 % of cases. These infants have small localized primary tumors with metastases to the liver, skin, or bone marrow that almost always spontaneously regress [4].

The overall prognosis of patients with NB has markedly improved, with 5-year survival rates increasing from 52 % from 1975 through 1977 to 74 % from 1999 through 2005,

according to the Surveillance, Epidemiology, and End Results databases (http://www.seer.cancer.gov). However, unlike the many childhood malignancies for which survival has been improved by recent therapies, high-risk NB is still one of the most difficult tumors to cure, with only 40 % long-term survival despite intensive multimodal therapy [1–3].

NBs are neuro-ectodermal tumors of embryonic neural crest-derived cells. The neural crest in normal development gives rise to nerve cells of the sympathetic nervous system. The fetal adrenal medulla consists of a mixture of chromaffin cells and clusters of mature ganglion cells; NBs most likely originate from a pluripotent precursor cell or from both these cell types, because NB tumors can contain cells with both neuronal and chromaffin cell phenotypes. NBs have various clinical outcomes, from spontaneous regression, caused by neuronal differentiation and/or apoptotic cell death, to malignant progression. The emerging patterns of multiple genetic abnormalities, such as aneuploidy, chromosomal gains and losses, and amplification of chromosomal material seem to mirror the different clinical entities and have led to better stratification of patients for therapy; however, despite many advances during the past three decades, NB has remained an enigmatic challenge to clinical and basic scientists.

Amplification of genomic DNA regions

MYCN oncogene

MYC, MYCN, and MYCL are helix-loop-helix/leucine zipper (HLH/LZ) proteins that form a heterodimer complex with MAX, which has high affinity for the consensus sequence CACGTG (E box MYC sites) and lower affinity for various non-canonical DNA sequences [5]. In the presence of growth factors, the expression of MYC family proteins has a positive role in cell-cycle progression [6]. However, normal cells with aberrant MYC expression are eliminated through apoptosis, although in cells having defects in the apoptosis machinery, deregulation of MYC may promote tumorigenesis.

Amplified *MYCN* in NBs is prototypic for the significance of proto-oncogene amplification in tumorigenesis [7, 8]. Amplified copies of *MYCN* can be present either extra-chromosomally as double minutes (DMs) or intra-chromosomally as homogeneously staining regions (HSRs). HSRs are generally located on different chromosomes, not at the resident site, 2p24, of *MYCN* [9]. Amplification values in NBs may range between 5- and more than 500-fold, and values of around 50- to 100-fold are usually seen in tumors. The complexity of amplified DNA encompassing *MYCN* can range from 100 kb to more than 1 Mb. A core 100- to 200-kb domain encompassing *MYCN* has been found consistently without rearrangements. The size of the DNA surrounding *MYCN* raises the possibility that additional genes may be co-amplified [10].

MYCN amplification occurs in roughly 20 % of primary NBs and is strongly correlated with advanced-stage disease [11] and treatment failure [12]. In localized NBs, *MYCN* amplification is the major prognostic factor, identifying patients who do not require aggressive therapy [13].

Extra copies of 17q

Gain of a long segment of the q-arm of chromosome 17 is associated with a poor outcome in NB [14]. The independent predictive power of the gain of 17q status was established in tumors with 17q, but without *MYCN* amplification or allelic losses of 1p or 11q [15]. It seems that unbalanced 17q gain identifies a larger population at risk than any other clinical or cytogenetic factor. The mechanism(s) involved in an adverse prognosis could be either the fusion of a gene flanking the 17q breakpoint, or a dosage effect of one or more genes in the extra 17q region. However, the breakpoint region is highly variable, which makes it very unlikely that just a single gene at 17q is involved in tumorigenesis; therefore, it is commonly thought that a dosage effect of one or more genes or a class of genes in the region of unbalanced gain is responsible for the altered phenotypes. The most prominent candidates implicated as having a role in NB progression in the common region of gain are *NM23-H1*, *NM23-H2* [16], and *SURVIVIN* [17].

Loss of genomic DNA regions

Allelic loss at 1p

One of the most prominent regions of loss of heterozygosity (LOH) in NBs is 1p, commonly identified in 30–35 % of all tumors. These deletions correlate not only with *MYCN* amplification, but also with an advanced disease stage [18]. In tumors with amplification of *MYCN*, LOH of 1p usually affects large areas, often reaching 1p32 or even more proximal. In contrast, the shortest region of overlap for 1p deletions in *MYCN* single-copy tumors was found to be smaller, and was defined at 1p36.3 [19, 20]. Despite intensive investigation, the gene or genes within chromosome 1p involved in NB tumorigenesis and aggressiveness remain to be elucidated. Whether the LOH due to deletion of alleles from 1p is an independent indicator of prognosis remains controversial. The different

regions of deletion associated with different biological entities suggest the existence of more than one tumor suppressor gene at chromosome 1p. Previous reports indicated that at least three discrete regions at chromosome 1p might be commonly deleted in NB, which suggests that these regions harbor putative tumor-suppressor genes [21]. Recent evidence indicates that *miR-34a*, a micro RNA (miRNA) known to regulate MYCN expression [22, 23], *CHD5* (1p36.31), a chromatin remodeling gene [24], and *KIF1bβ* (1p36.21), a pro-apoptotic gene [25], are candidate 1p36 NB tumor-suppressor genes.

Allelic loss of 11q

Allelic loss of 11q is present in 35–45 % of primary NBs [26, 27]. Notably, this genomic aberration is rarely seen in tumors with *MYCN* amplification, yet it remains highly associated with other high-risk features. Recently, loss of 11q has been reported to be highly correlated with adverse patient outcome [28], and has been proposed as a stratifying prognostic marker in the International Neuroblastoma Risk Group classification system [29], as well as in the upcoming clinical trial of the Children's Oncology Group. Previously, we performed array-comparative genomic hybridization (array-CGH) analysis for 236 primary NBs to search for genomic aberrations with high resolution. In our study, we have identified the shortest region of deletion overlap (10 Mb or less) at 11q23 [30]. Within this region, there exists a *TSLC1/IGSF4/CADM1* gene (tumor suppressor in lung cancer 1/immunoglobulin superfamily 4/cell adhesion molecule 1), and molecular and biological studies have suggested that TSLC1 acts as a candidate tumor suppressor gene for NB [31]. Recently, we have reported that MYCN induces polycomb BMI1, which suppresses 1p tumor suppressor KIF1bβ and 11q tumor suppressor TSLC1 epigenetically [32]. First, we studied BMI1 expression by Western blotting and found that the expression of the PRC1 complex protein BMI1 correlated with MYCN protein expression in NB cell lines and primary NB tumors. BMI1 induction by MYCN was at the miRNA level in an MYCN-inducible NB cell line and several other NB cell lines. *BMI1* promoter analysis by luciferase vector experiments determined an MYCN-binding E-box sequence in the promoter region, and chromatin immune-precipitation (ChIP) experiments confirmed direct binding of MYCN around the E-box region. Next, we transduced BMI1 in several NB cell lines by lentivirus vectors and found up-regulation of cell proliferation in vitro and in vivo. Consistent with this, *BMI1* knockdown using short hairpin (sh) RNAs produced by lentivirus vectors resulted in the induction of neurite elongation and the expression of the differentiation markers GAP43 and NF68. To understand how BMI1 controls NB cell proliferation and differentiation, we tried to identify the BMI1 target genes, except for *p14ARF/p16INK4a*, as we could not observe significant changes in these well-known tumor suppressors. To identify BMI1 target genes, except for *p14ARF* and *p16INK4a*, we performed expression gene profiling using an appropriate NB complementary DNA (cDNA) microarray (named the CCC-NHR13000 chip) carrying 13440 cDNA spots. Intriguingly, the well-known TSGs in NB–*TSLC1* (NM_014333.3) and *KIF1bβ* (AB017133)–are ranked as the first and second targets, respectively. We found that BMI1 expression considerably repressed *TSLC1* and *KIF1bβ* transcription in NB cells; by quantitative ChIP experiments, we addressed whether BMI1 specifically bound to *KIF1bβ* (ENSG 00000054523) and *TSLC1* (ENSG00000105767) promoter regions in NB cells. These findings, taken together, indicated an intriguing MYCN/BMI1/tumor-suppressor pathway in NB cells. This pathway might have a marked impact on NB tumorigenesis and is considered to be a target for the development of molecular-targeted therapy for refractory NBs.

Specific gene abnormality in neuroblastoma

High expression of the high-affinity receptor TrkA is found in mature sympathetic ganglia as well as in NBs with favorable prognosis. High TrkA expression is associated with younger age, lower stage, and absence of MYCN amplification. In contrast, low TrkA expression is associated with a poor prognosis and MYCN amplification [33, 34]. In contrast to TrkA and p75NTR, high expression of TrkB is preferentially found in high-risk tumors, particularly in those with amplification of MYCN [35].

The overall loss of caspase 8 (CASP8) expression in NBs is estimated to be 25–35 %, predominantly in high-risk tumors, and this loss seems to be strongly associated with the presence of amplified *MYCN* [36, 37]. The lack of CASP8 expression was associated with hypermethylation of a 5′-flanking sequence. The biological relevance of the loss of CASP8 follows from its central position in the extrinsic apoptotic route. CASP8 acts as a tumor suppressor gene, and inactivation will result in tumor cell survival.

Allelic loss at the short arm of chromosome 3 is a common event in many different cancers, including NBs. The shortest region of overlap in NBs has been defined at 3p25.3–3p14.3 [38]. *RASSF1A* (Ras-association domain family 1) is within the chromosomal 3p21.3 region and is frequently inactivated by hypermethylation in NB cell lines and tumors [39]. Hypermethylation of *RASSF1A* in NBs was reported in 40–55 % of tumors and 86 % of cell lines.

Genetic causes of familial neuroblastoma

Children with either sporadic or familial NBs in connection with congenital central hypoventilation syndrome, Hirschsprung's disease, or both, usually have loss-of-function mutations in the homeobox gene *PHOX2B* [40, 41].

It was recently reported that activating mutations in the tyrosine kinase domain of the anaplastic lymphoma kinase (*ALK*) oncogene account for most cases of hereditary NB [42]. These germ-line mutations encode for single-base substitutions in key regions of the kinase domain and result in constitutive activation of the kinase and a premalignant state. Mutations resulting in oncogene activation are also somatically acquired in 5–15 % of NBs [43–45].

Thus, genetic studies of mutations in *ALK* and *PHOX2B* should be considered whenever a patient has a family history of NB or has other clinical conditions that are strongly suggestive of a highly penetrant transmissible mutation, such as bilateral primary tumors of the adrenal glands.

DNA ploidy

Hyperdiploidy (gains and losses of one or more chromosomes of a diploid genome) is a form of genetic instability frequently observed in NBs. Different patterns of hyperdiploidy seem to be associated with different clinical entities. Near-diploid and near-tetraploid NBs are usually detected in patients over 1 year of age and are related to structural abnormalities involving allelic loss of chromosome 1p/amplification of the *MYCN* gene; these features are also related to aggressive tumors and a dismal outcome. Hyperdiploid or near-triploid NBs are usually found in patients under 12 months old or in low-risk tumors (stages 1, 2, and 4s) with few or no structural chromosomal abnormalities. Near-pentaploid NBs are rare and are found in patients with favorable prognostic factors and good prognosis [46]. The mechanisms leading to this type of genetic instability in NBs are still unclear.

Cancer stem cells in NB

The heterogeneity of NB tumor histology, which suggests the existence of a self-renewing multi-potent cancer stem cell in NB, was partially addressed in the study by Ross's group. This I-type cell appears to represent a more primitive stem cell, a progenitor of N- or S-type cells, capable of both self-renewal and bidirectional differentiation. I-type cells are significantly more malignant than N- or S-type cells, with four- to five-fold greater plating efficiencies in soft agar and six-fold higher tumorigenicity in athymic mice. Furthermore, a cancer stem cell-related marker, CD133, was highly expressed in I-type, but not in N- or S-type NB cells, suggesting the role of CD133 in stem cell-like phenotypes in I-type cells [47].

Recently, Kaplan's group indicated that dissociated cells from tumors or bone marrow grew as spheres under the conditions used to culture neural crest stem cells, and these spheres were capable of self-renewal, and exhibited chromosomal aberrations typical of NB. Primary spheres from all tumor risk groups differentiated under neurogenic conditions to form neurons. Impressively, as few as 10 passaged tumor sphere cells from aggressive NB injected orthotopically into severe combined immune-deficient/Beige mice formed large NB tumors that metastasized to several organs. Furthermore, highly tumorigenic tumor spheres were isolated from the bone marrow of patients in clinical remission, suggesting that this population of cells may predict clinical behavior and serve as a biomarker for minimal residual disease in high-risk patients [48].

Kaplan and colleagues have extended their work and identified compounds that selectively target patient-derived cancer stem cell-like tumor-initiating cells (TICs) while sparing normal pediatric stem cells (skin-derived precursors, SKPs), and they have characterized two therapeutic candidates, DECA-14 and rapamycin [49].

Further, to identify the signaling pathways important for the survival and self-renewal of NB TICs and potential therapeutic targets, they screened a small molecule library of 143 protein kinase inhibitors, including 33 in clinical trials. They indicated that PLK1 may be a candidate kinase that regulates TIC growth and survival, and they found that PLK1 inhibitors seem to be promising candidates as therapy for metastatic NB [50].

CD133 (prominin-1) was the first identified member of the prominin family of cell-surface glycoproteins harboring five transmembrane domains [51]. Importantly, CD133 is a marker of TICs in many cancers [52], and therefore it may be possible to develop future therapies towards targeting cancer stem cells via this marker. A previous report indicated that "I-type" cells, which have a significantly more malignant phenotype, with 4- to 5-fold greater plating efficiency in soft agar and six-fold higher tumorigenicity in athymic mice, expressed high amounts of *CD133* miRNA compared to less malignant sub-clones [47].

To address the role of CD133 in NB tumorigenesis, we transduced *CD133* cDNA or *CD133*-knocked down shRNA by lentivirus vector in NB cell lines and primary NB tumor spheres [53]. First, we knocked down *CD133* in highly expressing NB cells and analyzed the knockdown-induced phenotype. *CD133* knockdown in highly expressing NB cells effectively resulted in significant growth retardation in adherent cell culture/soft agar culture, and a significant reduction of xenograft tumor formation in

athymic mice. In concert, ectopic CD133 expression in CD133-low NB cells accelerated proliferation and colony formation in soft agar. In *CD133* knocked-down NB cells, neurite extension and GAP43/NF68 as neuronal differentiation markers were clearly up-regulated. Expression analysis of NB cell differentiation-related growth factor receptors/ligands in CD133-expressed or -reduced NB cells indicated that RET (rearranged during transfection of the proto-oncogene) transcription was suppressed by CD133. Additionally, in 20 NB cell lines and 12 unfavorable primary NB tumors derived from patients, RET expression was markedly repressed in CD133-expressing NB cells. CD133/RET co-expression abolished the inhibition of NB cell differentiation by CD133, which was caused by CD133-related activation of the p38 mitogen-activated protein kinase (MAPK) and phosphoinositide 3 kinase (PI3K)/Akt pathways. Intriguingly, *CD133* knockdown resulted in the inhibition of tumor sphere formation in both an NB cell line and primary tumor sphere-forming cells, suggesting that CD133 appears to have a role in tumor cell stemness in NBs, which is consistent with a previous report describing that CD133+ cells showed increased sphere formation and tumorigenicity in tumor sphere-forming LAN5 NB cells [54].

CD133 was previously characterized as having five alternative promoters (P1–P5) that are active in a tissue-dependent manner [55]. The P1, P2, and P3 promoters are located within a 1540-bp CpG island, whereas promoters P4 and P5 are not encompassed by CpG-rich sequences. We intend to study the CD133-expression mechanism in NB cells, including CD133 up-regulation in sphere-forming NB cells, because we observed a positive effect of CD133 on NB tumor sphere formation. Additionally, we detected the *CD133* promoter regions mainly working in NB cells. We analyzed the important promoter regions for CD133 expression in tumor sphere-forming NB cells because a significant increase was observed in the NB tumor spheres (data not shown). An increase of CD133 at the RNA and protein levels was achieved following demethylation, as determined by assays using 5-aza-2′-deoxycytidine (5-Aza-dC) [56]. The significance of CD133 promoter methylation in tumorigenesis in several tumors is still unresolved [57, 58].

Acknowledgments We thank Mr. Daniel Mrozek, Medical English Service, for editorial assistance. This work was supported in part by a Grant-in-Aid from the National Cancer Center Research and Development Fund of Japan (4), a Grant-in-Aid from the Ministry of Health, Labor, and Welfare of Japan for Third Term Comprehensive Control Research for Cancer, a Grant-in-Aid for Scientific Research (B) (24390269), and a Grant-in-Aid from the Uehara Memorial Foundation.

Conflict of interest We have no financial relationships to disclose.

References

1. Westermann F, Schwab M (2002) Genetic parameters of neuroblastomas. Cancer Lett 184:127–147
2. Maris JM, Hogarty MD, Bagatell R et al (2007) Neuroblastoma. Lancet 369:2106–2120
3. van Noesela MM, Versteeg R (2004) Pediatric neuroblastomas: genetic and epigenetic 'danse macabre'. Gene 325:1–15
4. D'Angio GJ, Evans AE, Koop CE (1971) Special pattern of widespread neuroblastoma with a favourable prognosis. Lancet 297:1046–1049
5. Kato GJ, Lee WM, Chen LL et al (1992) Max: functional domains and interaction with c-Myc. Genes Dev 6:81–92
6. Zindy F, Eischen CM, Randle DH et al (1998) Myc signaling via the ARF tumor suppressor regulates p53-dependent apoptosis and immortalization. Genes Dev 12:2424–2433
7. Kohl NE, Kanda N, Schreck RR et al (1983) Transposition and amplification of oncogene related sequence in human neuroblastomas. Cell 35:359–367
8. Schwab M, Alitalo K, Klempnauer KH et al (1983) Amplified DNA with limited homology to myc cellular oncogene is shared by human neuroblastoma cell lines and a neuroblastoma tumor. Nature 305:245–248
9. Corvi R, Amler LC, Savelyeva L et al (1994) MYCN is retained in single copy at chromosome 2 band p23–24 during amplification in human neuroblastoma cells. Proc Natl Acad Sci USA 91:5523–5527
10. Schwab M (1998) Amplification of oncogenes in human cancer cells. Bioessays 20:473–479
11. Seeger RC, Brodeur GM, Sather H et al (1985) Association of multiple copies of the N-myc oncogene with rapid progression of neuroblastomas. N Engl J Med 313:1111–1116
12. Brodeur G, Seeger RC, Schwab M et al (1984) Amplification of N-myc in untreated human neuroblastomas correlates with advanced disease stage. Science 224:1121–1124
13. Rubie H, Hartmann O, Michon J et al (1997) Localized neuroblastoma: MYCN amplification is the main prognostic factor-results of the NBL 90 study. J Clin Oncol 15:1171–1182
14. Caron H (1995) Allelic loss of chromosome 1 and additional chromosome 17 material are both unfavourable prognostic markers in neuroblastoma. Med Pediatr Oncol 24:215–221
15. Bown N, Cotterill S, Lastowska M et al (1999) Gain of chromosome arm 17q and adverse outcome in patients with neuroblastoma. N Engl J Med 340:1954–1961
16. Okabe-Kado J, Kasukabe T, Honma Y et al (2005) Clinical significance of serum NM23-H1 protein in neuroblastoma. Cancer Sci 96:653–660
17. Adida C, Berrebi D, Peuchmaur M et al (1998) Anti-apoptosis gene, survivin, and prognosis of neuroblastoma. Lancet 351:882–883
18. White PS, Maris JM, Beltinger C et al (1995) A region of consistent deletion in neuroblastoma maps within 1p36.2-3. Proc Natl Acad Sci USA 92:5520–5524
19. Caron H, Spieker N, Godfried M et al (2001) Chromosome bands 1p35–36 contain two distinct neuroblastoma tumor suppressor loci, one of which is imprinted. Genes Chromosom Cancer 30:168–174
20. Bauer A, Savelyeva L, Claas A et al (2001) Smallest region of overlapping deletion in 1p36 in human neuroblastoma: a 1 Mbp cosmid and PAC contig. Genes Chromosom Cancer 31:228–239
21. Brodeur GM (2003) Neuroblastoma: biological insights into a clinical enigma. Nat Rev Cancer 3:203–216
22. Wei JS, Song YK, Durinck S et al (2008) The MYCN oncogene is a direct target of miR-34a. Oncogene 27:5204–5213

23. Cole KA, Attiyeh EF, Mosse YP et al (2008) A functional screen identifies miR-34a as a candidate neuroblastoma tumor suppressor gene. Mol Cancer Res 6:735–742
24. Bagchi A, Papazoglu C, Wu Y et al (2007) CHD5 is a tumor suppressor at human 1p36. Cell 128:459–475
25. Munirajan AK, Ando K, Mukai A et al (2008) KIF1Bbeta functions as a haploinsufficient tumor suppressor gene mapped to chromosome 1p36.2 by inducing apoptotic cell death. J Biol Chem 283:24426–24434
26. Guo C, White PS, Weiss MJ et al (1999) Allelic deletion at 11q23 is common in MYCN single copy neuroblastomas. Oncogene 18:4948–4957
27. Spitz R, Hero B, Ernestus K et al (2003) Deletions in chromosome arms 3p and 11q are new prognostic markers in localized and 4s neuroblastoma. Clin Cancer Res 9:52–58
28. Attiyeh EF, London WB, Mosse YP et al (2005) Chromosome 1p and 11q deletions and outcome in neuroblastoma. N Engl J Med 353:2243–2253
29. Cohn SL, Pearson AD, London WB et al (2009) The International Neuroblastoma Risk Group (INRG) classification system: an INRG Task Force report. J Clin Oncol 27:289–297
30. Tomioka N, Oba S, Ohira M et al (2008) Novel risk stratification of patients with neuroblastoma by genomic signature which is independent of molecular signature. Oncogene 27:441–449
31. Ando K, Ohira M, Ozaki T et al (2008) Expression of TSLC1, a candidate tumor suppressor gene mapped to chromosome 11q23, is downregulated in unfavorable neuroblastoma without promoter hypermethylation. Int J Cancer 123:2087–2094
32. Ochiai H, Takenobu H, Nakagawa A et al (2010) Bmi1 is a MYCN target gene and regulates tumorigenesis via repression of KIF1Bβ and TSLC1 in neuroblastoma. Oncogene 29:2681–2690
33. Kogner P, Barbany G, Dominici C et al (1993) Coexpression of messenger RNA for TRK protooncogene and low affinity nerve growth factor receptor in neuroblastoma with favorable prognosis. Cancer Res 53:2044–2050
34. Nakagawara A, Arima-Nakagawara M, Scavarda NJ et al (1993) Association between high levels of expression of the TRK gene and favorable outcome in human neuroblastoma. N Engl J Med 328:847–854
35. Nakagawara A, Azar CG, Scavarda NJ et al (1994) Expression and function of TRK-B and BDNF in human neuroblastomas. Mol Cell Biol 14:759–767
36. Eggert A, Grotzer MA, Zuzak TJ et al (2001) Resistance to tumor necrosis factor-related apoptosis-inducing ligand (TRAIL)-induced apoptosis in neuroblastoma cells correlates with a loss of caspase-8 expression. Cancer Res 61:1314–1319
37. Teitz T, Wei T, Valentine MB et al (2000) Caspase 8 is deleted or silenced preferentially in childhood neuroblastomas with amplification of MYCN. Nat Med 6:529–535
38. Ejeskar K, Aburatani H, Abrahamsson J et al (1998) Loss of heterozygosity of 3p markers in neuroblastoma tumours implicate a tumour-suppressor locus distal to the FHIT gene. Br J Cancer 77:1787–1791
39. Astuti D, Agathanggelou A, Honorio S et al (2001) RASSF1A promoter region CpG island hypermethylation in phaeochromocytomas and neuroblastoma tumours. Oncogene 20:7573–7577
40. Mosse YP, Laudenslager M, Khazi D et al (2004) Germline PHOX2B mutation in hereditary neuroblastoma. Am J Hum Genet 75:727–730
41. Trochet D, Bourdeaut F, Janoueix-Lerosey I et al (2004) Germline mutations of the paired-like homeobox 2B (PHOX2B) gene in neuroblastoma. Am J Hum Genet 74:761–764
42. Mossé YP, Laudenslager M, Longo L et al (2008) Identification of ALK as a major familial neuroblastoma predisposition gene. Nature 455:930–935
43. Janoueix-Lerosey I, Lequin D, Brugières L et al (2008) Somatic and germline activating mutations of the ALK kinase receptor in neuroblastoma. Nature 455:967–970
44. George RE, Sanda T, Hanna M et al (2008) Activating mutations in ALK provide a therapeutic target in neuroblastoma. Nature 455:975–978
45. Chen Y, Takita J, Choi YL et al (2008) Oncogenic mutations of ALK kinase in neuroblastoma. Nature 455:971–974
46. Look AT, Hayes FA, Shuster JJ et al (1991) Clinical relevance of tumor cell ploidy and N-myc gene amplification in childhood neuroblastoma: a Pediatric Oncology Group study. J Clin Oncol 9:581–591
47. Walton JD, Kattan DR, Thomas SK et al (2004) Characteristics of stem cells from human neuroblastoma cell lines and in tumors. Neoplasia 6:645–838
48. Hansford LM, McKee AE, Zhang L et al (2007) Neuroblastoma cells isolated from bone marrow metastases contain a naturally enriched tumor-initiating cell. Cancer Res 67:11234–11243
49. Smith KM, Datti A, Fujitani M et al (2010) Selective targeting of neuroblastoma tumour-initiating cells by compounds identified in stem cell-based small molecule screens. EMBO Mol Med 2:371–384
50. Grinshtein N, Datti A, Fujitani M et al (2011) Small molecule kinase inhibitor screen identifies polo-like kinase 1 as a target for neuroblastoma tumor-initiating cells. Cancer Res 71:1385–1395
51. Corbeil D, Fargeas CA, Huttner WB (2001) Rat prominin, like its mouse and human orthologues, is a pentaspan membrane glycoprotein. Biochem Biophys Res Commun 285:939–944
52. O'Brien CA, Kreso A, Jamieson CHM (2010) Cancer stem cells and self-renewal. Clin Cancer Res 16:3113–3120
53. Takenobu H, Shimozato O, Nakamura T et al (2011) CD133 suppresses neuroblastoma cell differentiation via signal pathway modification. Oncogene 30:97–105
54. Mahller YY, Williams JP, Baird WH et al (2009) Neuroblastoma cell lines contain pluripotent tumor initiating cells that are susceptible to a targeted oncolytic virus. PLoS ONE 4:e4235
55. Shmelkov SV, Jun L, St Clair R et al (2004) Alternative promoters regulate transcription of the gene that encodes stem cell surface protein AC133. Blood 103:2055–2061
56. Schiapparelli P, Enguita-Germán M, Balbuena J et al (2010) Analysis of stemness gene expression and CD133 abnormal methylation in neuroblastoma cell lines. Oncol Rep 24:1355–1362
57. Baba T, Convery PA, Matsumura N et al (2009) Epigenetic regulation of CD133 and tumorigenicity of CD133+ ovarian cancer cells. Oncogene 28:209–218
58. Yi JM, Tsai HC, Glöckner SC et al (2008) Abnormal DNA methylation of CD133 in colorectal and glioblastoma tumors. Cancer Res 68:8094–8103

Published OnlineFirst July 19, 2012; DOI:10.1158/0008-5472.CAN-12-0943

Cancer Research

NLRR1 Enhances EGF-Mediated *MYCN* Induction in Neuroblastoma and Accelerates Tumor Growth *In Vivo*

Shamim Hossain, Atsushi Takatori, Yohko Nakamura, et al.

Cancer Res 2012;72:4587-4596. Published OnlineFirst July 19, 2012.

Published OnlineFirst July 19, 2012; DOI:10.1158/0008-5472.CAN-12-0943

Cancer Research

NLRR1 Enhances EGF-Mediated *MYCN* Induction in Neuroblastoma and Accelerates Tumor Growth *In Vivo*

Shamim Hossain[1], Atsushi Takatori[1], Yohko Nakamura[1], Yusuke Suenaga[1], Takehiko Kamijo[2], and Akira Nakagawara[1]

Abstract

Neuronal leucine-rich repeat protein-1 (NLRR1), a type-1 transmembrane protein highly expressed in unfavorable neuroblastoma, is a target gene of MYCN that is predominately expressed in primary neuroblastomas with *MYCN* amplification. However, the precise biological role of NLRR1 in cell proliferation and tumor progression remains unknown. To investigate its functional importance, we examined the role of NLRR1 in EGF and insulin growth factor-1 (IGF-1)–mediated cell viability. We found that NLRR1 positively regulated cell proliferation through activation of extracellular signal–regulated kinase mediated by EGF and IGF-1. Interestingly, EGF stimulation induced endogenous *MYCN* expression through Sp1 recruitment to the *MYCN* promoter region, which was accelerated in NLRR1-expressing cells. The Sp1-binding site was identified on the promoter region for *MYCN* induction, and phosphorylation of Sp1 was important for EGF-mediated MYCN regulation. *In vivo* studies confirmed the proliferation-promoting activity of NLRR1 and established an association between *NLRR1* expression and poor prognosis in neuroblastoma. Together, our findings indicate that NLRR1 plays an important role in the development of neuroblastoma and therefore may represent an attractive therapeutic target for cancer treatment. *Cancer Res; 72(17); 4587–96. ©2012 AACR.*

Introduction

Neuroblastoma is one of the most common extracranial malignant tumors that develop in children; they arise from neural crest cells and are mostly found in the adrenal medulla or along the sympathetic chain (1). neuroblastoma exhibits clinical and biological heterogeneity, ranging from rapid progression associated with metastatic spread and poor clinical outcome to occasional, spontaneous, or therapy-induced regression or differentiation into benign ganglioneuroma (2, 3). Different subsets of neuroblastoma show various distinct genetic features, including DNA ploidy, *MYCN* amplification, allelic loss of the distal part of chromosome 1p, and gain of chromosome 17q (4). Amplification of the *MYCN* gene usually distinguishes a subset of neuroblastoma with poor prognosis (1), and recovery of children with high-risk neuroblastoma remains low, providing a compelling reason for better understanding of the molecular mechanisms that can be targeted to treat this disease (5, 6). *MYCN* transgenic mice develop neuroblastoma, which implicates that MYCN can maintain the tumorigenic state, supporting the importance of the *MYCN* gene as a potential therapeutic target (7–9). However, the precise mechanism of *MYCN* regulation and the functional correlation with other proteins in the progression of neuroblastoma are still elusive.

NLRR1 is a type I transmembrane protein with extracellular leucine-rich repeats, and belongs to the mammalian neuronal leucine-rich protein family (NLRR1–NLRR5; ref. 10–13). We previously reported that mRNA expression levels of *NLRR1* are significantly higher in unfavorable neuroblastoma (12). We further reported that NLRR1 protein expression is higher in *MYCN*-amplified primary neuroblastomas than in nonamplified tumors, and that MYCN can transcriptionally upregulate *NLRR1* (14). We also found that overexpression of NLRR1 promoted neuroblastoma cell proliferation and inhibited cellular apoptosis upon serum starvation (14). NLRR family proteins have also been considered as cell adhesion or signaling molecules, and mouse NLRR3 functions in EGF-mediated activation of extracellular signal–regulated kinase (ERK; ref. 15).

EGF signaling was reported to be involved in neuroblastoma cell proliferation via the activation of ERK and AKT (16). Insulin growth factor-I (IGF-I) stimulation was also reported to enhance neuroblastoma cell proliferation, and is involved in the induction of *MYCN* expression through mitogen-activated protein kinase (MAPK; ref. 17). MAPK kinase (MKK) proteins are crucially important in several cellular events, including proliferation, survival, and differentiation (18, 19). Several stimuli activate MKKs, which is followed by activation of MAPKs, including ERK, JNK, and p38 MAPK. Abnormalities in MAPK pathways, especially mutations of proteins of these signaling cascades, have been reported in about 20% of all

Authors' Affiliations: Divisions of [1]Biochemistry & Innovative Cancer Therapeutics and [2]Biochemistry and Molecular Carcinogenesis, Chiba Cancer Center Research Institute, Chiba, Japan

Note: Supplementary data for this article are available at Cancer Research Online (http://cancerres.aacrjournals.org/)

Corresponding Author: Akira Nakagawara, Division of Biochemistry & Innovative Cancer Therapy, Chiba Cancer Center Research Institute, 666-2 Nitona, Chuoh-ku, Chiba 260-8717, Japan. Phone: 81-43-264-5431; Fax: 81-43-265-4459; E-mail: akiranak@chiba-cc.jp

doi: 10.1158/0008-5472.CAN-12-0943

Published OnlineFirst July 19, 2012; DOI:10.1158/0008-5472.CAN-12-0943

human cancers (20, 21). Several reports suggest that MKK/ERK signaling has an important role in tumorigenesis and metastasis (22–24). However, the precise role of MKK/ERK signaling in the development of neuroblastoma and its functional relationship with *MYCN* oncogene are still unknown. NLRR1 is a possible regulator of growth factor signaling, and may play a crucial role in *MYCN*-amplified neuroblastoma to form aggressive tumors. In this study, we report that EGF promotes ERK activation and is involved in *MYCN* induction via recruitment of Sp1 to the *MYCN* promoter. Overexpression of NLRR1 enhanced *MYCN* induction by activating ERK signaling, whereas knockdown of *NLRR1* suppressed ERK phosphorylation and *MYCN* induction upon EGF treatment. *In vivo* studies in nude mice showed significant tumorigenic activity of NLRR1. Our present findings collectively indicate that NLRR1 accelerates growth factor signaling to induce *MYCN*, and plays a positive feedback loop with MYCN to induce aggressive tumor progression in neuroblastoma.

Materials and Methods

Cell lines, transfection, and reagents

Human neuroblastoma-derived SK-N-BE and SH-SY5Y cells were collected from CHOP cell lines and were maintained in RPMI 1640 medium supplemented with 10% heat-inactivated fetal bovine serum (Invitrogen), 50 μg/mL penicillin, and 50 μg/mL streptomycin (Invitrogen). Cells were cultured in a humidified atmosphere of 5% CO^2 and 95% air at 37°C. For transient transfection, SK-N-BE cells were transfected with the indicated plasmids using Lipofectamine 2000 (Invitrogen) according to the manufacturer's instructions.

Cell proliferation assays

SK-N-BE and SH-SY5Y cell proliferation was evaluated using the tetrazolium compound WST-8 (Cell Counting Kit-8 Dojindo Laboratories, Japan). Cell proliferation was determined according to the manufacturer's instructions.

RNA extraction and reverse transcription-PCR

Total RNA was prepared from the indicated cells using the RNeasy Mini Kit (Qiagen) according to the manufacturer's protocol, and reverse-transcription was performed. The specific primers used were as follows: *MYCN*, 5′-CTTCGGTCCAGCTTTCTCAC-3′ and 5′-GTCCGAGCGTGTTCAATTTT-3′; NLRR1, 5-GCAGCTTTTCAACTTGACTGAA-3 and 5-TGCAGCAGCTTTTCAACTTGACTGAAC-3; *VEGF*, 5′-AAGGAGGAGGGCAGAATCAT-3′ and 5′-ATCTGCATGGTGATGTTGGA-3′; *Sp1*, 5′-TGCAGCAGAATTGAGTCACC -3′ and 5′- CACAACATACTGCCCACCAG-3′; *GAPDH*, 5′- ACCTGACCTGCCGTCTAGAA-3′ and 5′-TCCACCACCCTGTTGCTGTA-3′. *GAPDH* expression was measured as an internal control.

Immunoblotting

Cells were collected and washed with PBS. Whole cell lysates were prepared by incubating cells in lysis buffer containing 10 mmol/L Tris-HCl, pH 8.0, 150 mmol/L NaCl, 2 mmol/L ethyleneglycol tetraacetic acid, 50 mmol/L β-mercaptoethanol, 1% Triton X-100, a commercial protease inhibitor mixture (Sigma), and phosphatase inhibitor mixture (Sigma), for 30 minutes on ice, and subjected to brief sonication for 10 seconds at 4°C, followed by centrifugation at 15,000 rpm at 4°C for 10 minutes to remove insoluble materials. Protein concentration was measured using the BCA Protein Assay Kit (Thermo Scientific) according to the manufacturer's instruction. Equal amounts of protein (50 μg) were separated by 7.5% SDS-PAGE and electrophoretically transferred onto polyvinylidene difluoride (PVDF) membranes (Immobilion-P, Millipore. PVDF membranes were then blocked with TBS containing 5% nonfat dry milk and 0.1% Tween 20 at room temperature for 1 hour. After blocking, the membranes were incubated at 4°C overnight with anti-MYCN (Ab-1, Oncogene), anti-EGFR (Rockland), anti-actin (20–33; Sigma), and other antibodies against ERK1/2, phospho-ERK, IGF1R, phospho IGFR1, Akt, phospho-Akt, and phospho-EGFR were purchased from Cell Signaling Technology. After incubation with primary antibodies, membranes were incubated with horseradish peroxidase-coupled goat anti-mouse or anti-rabbit IgG secondary antibody (Cell Signaling Technology) for 1 hour at room temperature. Immunoblots were visualized using ECL detection reagents according to the manufacturer's instruction (Amersham Biosciences).

Construction of luciferase reporters

A luciferase reporter construct driven by the *MYCN* promoter was generated by using the following primer sets: MYCN (−221/+21), 5′- GAGCTCCAGCTTTGCAGCCTTCTC-3′ and 5′- GAGCTCGTCCAGACAGATGACTGTC-3′. Underlined sequences indicate *SacI* enzyme recognition sites. Then, the PCR product was inserted into the *SacI* site of pGL3 basic vector. Mutation of the 2 putative Sp1-binding sites was performed using a site-directed mutagenesis kit (Promega) using the following primer sets: mut-1 (−221/+21), 5′-ACAGCCCCCTTCTCTCCCC(A)G(A)CCC(A)CCCGG-3′(sense), 5′-GGGAGAGAAGGGGGCTGTGGCGCA-3′ (antisense); mut-2 (−221/+21), 5′-ATGGAAATCAGGAGGGC(A)G(A)GGGTAAAG-3′(sense), 5′-CCCTCCTGATTTCCATAAAAATCA-3′ (antisense). Underlined sequences represent putative Sp1-binding sites, and the mutated nucleotides are marked by brackets.

Luciferase reporter assays

SK-N-BE cells were plated in 12-well plates at a density of 50,000 cells/well, and transiently transfected with reporter constructs driven by the *MYCN* promoter (200 ng) and pRL-TK *Renilla* luciferase reporter plasmid (20 ng). After the indicated time periods, cells were collected and washed with PBS, and their luciferase activities were measured using a luciferase reporter assay system (Promega). Each experiment was performed at least 3 times in triplicate.

siRNA transfection

A mixture of 2 siRNAs with antisense sequences of 5′-UCUUGGUUGAGCUGUGUAGTT-3′ and 5′-UUGUGGACACUCACUAUUCTT-3′ were designed to target human *NLRR1* (TAKARA). Control siRNA was purchased from Ambion (Cat 4635). SK-N-BE cells were transfected with 20 nmol/L of the indicated siRNAs using Lipofectamine RNAiMAX (Invitrogen).

Published OnlineFirst July 19, 2012; DOI:10.1158/0008-5472.CAN-12-0943

ChIP assays

Before collection, cells were cross-linked with 1% formaldehyde in medium for 10 minutes at 37°C. Chromatin immunoprecipitation (ChIP) was performed following the protocol provided by Upstate Biotechnology. In short, cross-linked chromatin was prepared from cells and sonicated to an average length of 200 to 800 nucleotides, precleaned with protein A-agarose beads pretreated with shared salmon sperm DNA, and immunoprecipitated with rabbit anti-E2F1 (KH95, Santa Cruz) and rabbit anti-Sp1 (DAM1718081, Upstate/Millipore) antibodies conjugated with protein A-agarose. The immunoprecipitates were eluted with 100 μL elution buffer (1% SDS and 0.1 mol/L $NaHCO_3$). Formaldehyde-mediated cross-links were reversed by heating at 65°C for 4 hours, and the reaction mixtures were treated with proteinase K at 45°C for 1 hour. Precipitated DNA and control input DNA were purified using a QIAquick PCR Purification Kit (Qiagen). Purified DNA was amplified by PCR using the following primer set: 5′- CAGCTTTGCAGCCTTCTC-3′ and 5′-GTCCAGACAGATGACTGTC-3′ targeting the MYCN core promoter region (−221, +21).

Animals and tumor xenograft studies

Male BALB/c athymic (nu/nu) mice (5–6 weeks old) were purchased from Japan SLC, and maintained under specific pathogen-free conditions strictly following the Chiba Cancer Center Research Institute guidelines. Stably expressing NLRR1 and mock SH-SY5Y cell lines were established by transfection followed by selection with G418 at a concentration of 600 μg/mL for about 6 to 8 weeks. Single colonies were picked to confirm the ectopic expression of NLRR1. Three NLRR1-expressing clones were used for the tumor xenograft studies, and 3 mock-transfected single clones were used as negative controls. A total of 6 groups of mice (7 mice in each group) received subcutaneous injections of 1×10^7 cells dissolved in 100 μL PBS. The length and width of each tumor was recorded each week at the indicated time periods. Tumor volume was calculated according the following formula: [length × $(\text{width})^2$]/2 (25, 26). Survival curves were generated using the Kaplan–Meier method using SPSS software. Log-rank tests were performed to calculate the *P* value between the 2 survival curves.

Immunohistochemical staining

To prepare the cryosections, tumors were fixed in 4% paraformaldehyde, washed with sucrose solution, embedded in OCT compound, frozen, and sectioned at 10 μm thickness. Sections were air-dried, washed with TBS, blocked in Mouse on Mouse blocking solution (MOM; PK-2200, Vector Laboratories) with 5% goat serum and 2% bovine serum albumin, and then treated with MOM diluent. Sections were then incubated with anti-NLRR1 (TB776, affinity purified, MBL) and anti-Ki-67 (mouse monoclonal 556003, BD) antibodies. MOM anti-mouse IgG and rabbit Alexa 488 were used as secondary antibodies followed by Fluorescein Avidin CY3 (Vector Laboratories). DAPI was used to stain the nuclei.

Four-mm thick paraffin tissue sections of the mock and NLRR1 tumors were subjected to immunohistochemistry (IHC). After deparafinization antigen retrieval was performed by boiling with 0.1 mol/L citrate buffer (pH 6.0) using microwave at 800 W for 10 minutes. The primary antibody for NMYC (Ab-1, Oncogene), p-ERK (4376, Cell signaling), and ERK (4695, Cell signaling) was used at 1:100 dilutions followed by the

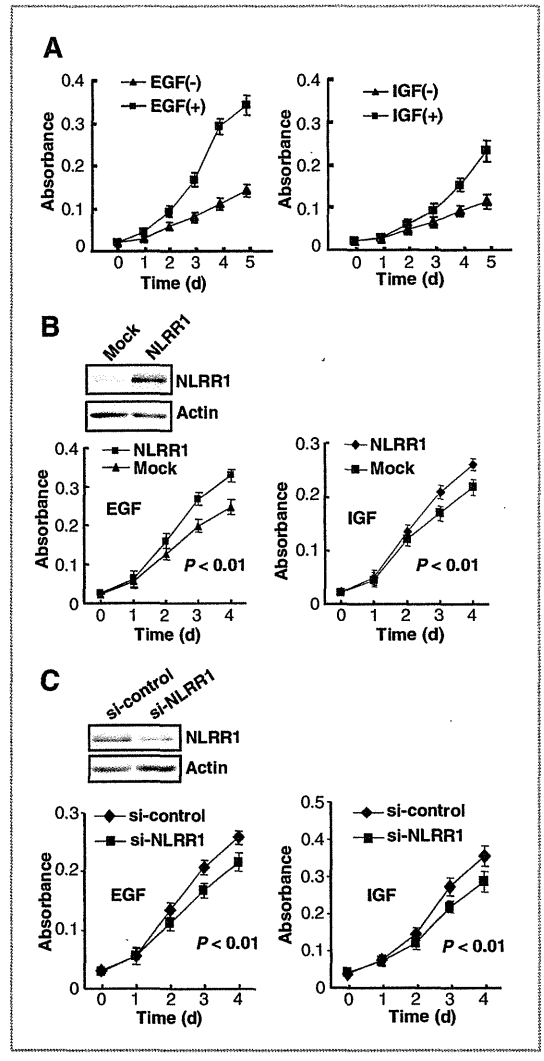

Figure 1. NLRR1 promotes EGF/IGF-mediated cell proliferation. A, quantification of SK-N-BE cell proliferation following EGF (left) and IGF (right) stimulation for the indicated time periods using WST-8 assays. The data are represented as mean ± SD. B, ectopic expression of NLRR1 in SK-N-BE cells was confirmed by immunoblotting (top). NLRR1-expressing SK-N-BE cells were treated with EGF (left) and IGF (right) for the indicated time periods, and proliferation was measured by WST-8 assays. C, NLRR1 knockdown by transfection with siRNA was confirmed by immunoblotting (top). Growth curve of SK-N-BE cells transfected with control siRNA and siRNA against NLRR1 in the presence of EGF (left) and IGF (right) was measured by WST-8 assays. For all WST-8 assays (A, B, and C), cells were cultured in 2% serum-containing medium, and growth factors were used at a concentration of 50 ng/mL.

Published OnlineFirst July 19, 2012; DOI:10.1158/0008-5472.CAN-12-0943

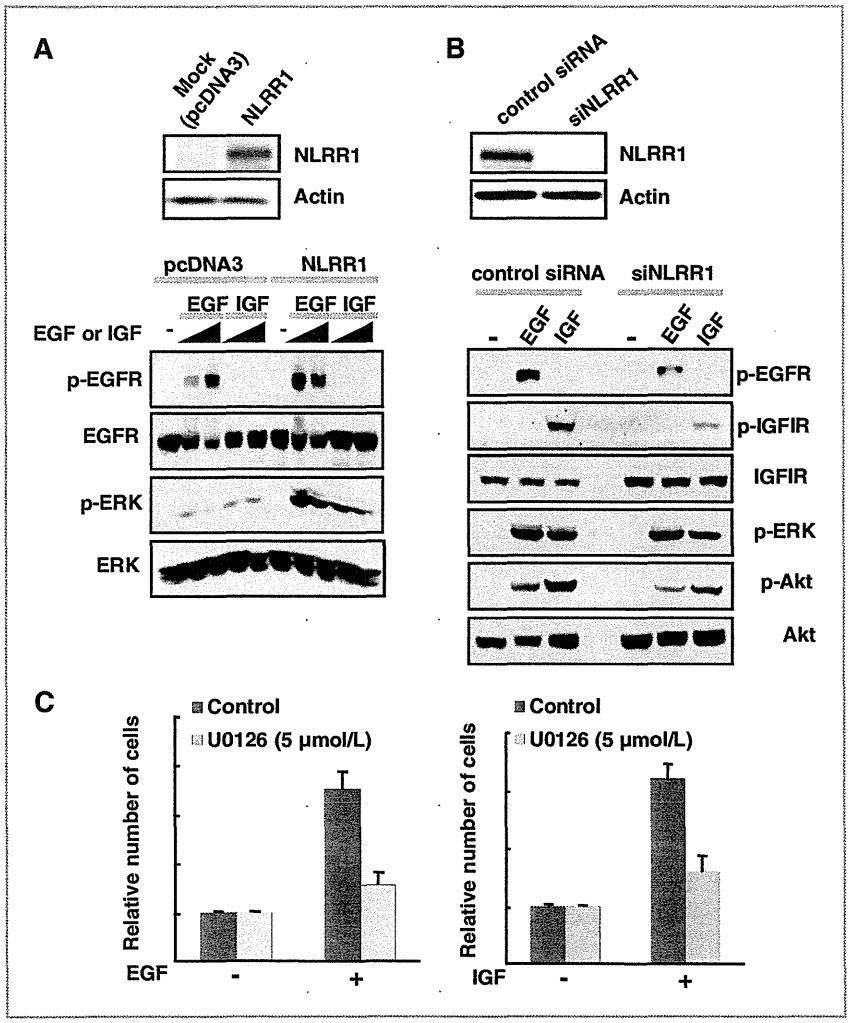

Figure 2. NLRR1 enhances EGF and IGF-mediated phosphorylation of ERK. A, SK-N-BE cells were transiently transfected with mock (pCDNA3) and NLRR1-expressing plasmid. Forty-eight hours after transfection, cells were starved with serum-free medium for 12 hours and then stimulated with EGF and IGF for 10 minutes. Whole cell lysates were used for immunoblotting with specific antibodies (bottom). NLRR1 overexpression was confirmed by immunoblotting of the same lysates (top). B, siRNA-mediated knockdown of NLRR1 suppresses phosphorylation of ERK mediated by EGF and IGF (bottom). The experimental conditions are similar to those in A. Knockdown efficiency was confirmed by immunoblotting (top). C, SK-N-BE cells transfected with NLRR1-expressing plasmids were pretreated with MEK1/2-specific inhibitor (U0126) and then cultured in the presence or absence of EGF and IGF; cell proliferation was measured by WST-8 assays.

standard protocol of Cell signaling. Secondary biotinylated universal antibody from Vector Laboratories was applied at a dilution of 1:400. Reactivity was visualized with an avidin-biotin complex immunoperoxidase system using diaminobenzidine as the chromagen and Hematoxylin as the counterstain (Vector Laboratories).

Results

NLRR1 enhances EGF/IGF-mediated cell proliferation in neuroblastoma cells

Our previous report showed that *NLRR1* is a direct transcriptional target of MYCN in neuroblastoma, and is associated with cell proliferation and survival (14). However, the mechanism by which NLRR1 regulates cell proliferation was still unknown. Another member of leucine rich repeat protein family, NLRR3, has been associated with the activation of ERK (15), and EGFR activation was reported to accelerate neuroblastoma cell proliferation (16), suggesting the possibility that NLRR1 may activate EGFR to induce cell proliferation. To test this hypothesis, we first investigated neuroblastoma cell proliferation upon EGF and IGF-I treatment. Consistent with their proliferative role (16, 17), both EGF and IGF-I also accelerated the proliferation of SK-N-BE cells (Fig. 1A). Similar data were also observed in neuroblastoma SH-SY5Y cells (data not shown). To determine whether NLRR1 promotes EGF- and IGF-1–mediated cell proliferation, we transiently transfected SK-N-BE cells with NLRR1 expression plasmid and treated them with EGF and IGF-I. Interestingly, ectopic expression of NLRR1 enhanced the cell proliferation mediated by EGF and IGF-I (Fig. 1B). Overexpression of NLRR1 in SH-SY5Y showed similar promotion of proliferation (data not shown). To confirm the role of NLRR1, we used an RNA interference approach to knock down endogenous *NLRR1*. The data suggested that knockdown of *NLRR1* suppressed the EGF- and IGF-1–mediated cell proliferation (Fig. 1C). Collectively, the data suggested

Published OnlineFirst July 19, 2012; DOI:10.1158/0008-5472.CAN-12-0943

that NLRR1 enhances cell proliferation mediated by EGF and IGF-I.

NLRR1 enhances EGF and IGF-mediated activation of ERK

Because ERK is an important kinase that is often regulated by EGF and IGF-1 growth factors to induce cell proliferation, we were interested to determine whether NLRR1 affected ERK phosphorylation upon EGF and IGF-I treatment. We examined the activation of ERK in NLRR1-overexpressing cells. Interestingly, ERK phosphorylation was enhanced compared with the mock-transfected cells (Fig. 2A). The increased phosphorylation of EGFR was observed in the NLRR1 overexpressing SK-N-BE cells upon EGF stimulation (Fig. 2A). Similar data were also observed in SH-SY5Y cells (data not shown). We also used siRNA studies to further elucidate the role of NLRR1 in EGF and IGF-1 signaling. Consistent with the overexpression study, we observed a reduction in ERK phosphorylation in *NLRR1* knockdown cells upon both EGF and IGF-1 treatment compared with the control siRNA-transfected cells (Fig. 2B). Interestingly, phosphorylation of EGFR and IGFR was found to be decreased in NLRR1 knockdown cells (Fig. 2B). To elucidate whether the activation of ERK is important for cell proliferation, we used the MEK1/2-specific inhibitor, U0126 (27), in the cell proliferation assays. For the cell proliferation assays, we have used the minimum concentration of U0126 (5 μmol/L) required to inhibit ERK activation in the cells (Supplementary Fig. S1). The data showed that EGF- and IGF-I–mediated proliferation of NLRR1-overexpressing SK-N-BE cells was inhibited upon U0126 treatment (Fig. 2C).

EGF stimulation induces *MYCN* via ERK

IGF-I stimulation induces endogenous *MYCN* expression in neuroblastoma cells via MAPK activation (17). Therefore, it is possible that EGF can induce *MYCN*, because EGF treatment also activates MAPK. To investigate this hypothesis, we treated SK-N-BE cells cultured in serum-free medium with increasing amounts of EGF. Consistent with our hypothesis, both mRNA and protein levels of MYCN were induced upon EGF treatment (Fig. 3A). Time course experiments were also used to confirm that EGF can induce *MYCN*. *MYCN* was found to be induced at 6 hours after EGF treatment (Fig. 3B). Under our experimental conditions, EGF treatment successfully phosphorylated EGFR (Supplementary Fig. S1) and ERK (data not shown). We also observed that EGF stimulation induced *MYCN* expression in other neuroblastoma cell lines, SH-SY5Y and NLF (data not shown). To verify our experimental data that EGF induces *MYCN*, we used *VEGF* as positive control, which was reported to be induced by EGF (28). AG1478 is a specific inhibitor for EGFR, and is sufficient to block EGFR-mediated activation of ERK (29, 30). We have confirmed the effect of the optimum concentration of AG1478 to inhibit EGF-mediated phosphorylation of EGFR in the cells (Supplementary Fig. S1). Therefore, we used the optimum concentrations of AG1478 to elucidate that EGF-mediated *MYCN* induction is dependent on EGFR-ERK signaling. Consistently, *MYCN* induction by EGF was successfully blocked in AG1478-pretreated SK-N-BE cells (Fig. 3C left). We also used U0126 to prove that EGF-mediated *MYCN* induction is dependent on ERK (Fig. 3C, right panel). These data collectively suggest that EGF-mediated *MYCN* induction is dependent on the EGFR–ERK pathway in neuroblastoma cells.

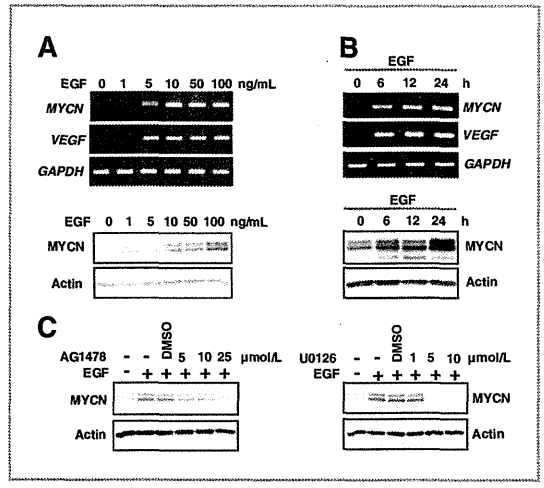

Figure 3. EGF stimulation induces endogenous *MYCN*. A, serum-starved SK-N-BE cells were treated with increasing doses of EGF for 12 hours. Total mRNA was used in reverse transcription (RT)-PCR to check the expression of *MYCN* and *VEGF* (top). *GAPDH* was checked as an internal control. Whole cell lysates were used in immunoblotting to detect the proteins (bottom). B, MYCN was induced by EGF in a time-dependent manner. Serum-starved SK-N-BE cells were treated with 50 ng/mL of EGF. Total RNA and whole cell lysates were collected at the indicated time points for RT-PCR (top) and Western blotting (bottom) assays to check the expression level of MYCN. C, SK-N-BE cells were cultured in serum-free medium for 12 hours with or without different concentrations of AG1478 (left) and U0126 (right). Cells were then treated with EGF (50 ng/mL) for 12 hours, and whole cell lysates were used to check MYCN protein levels by immunoblotting. Actin was checked as an internal control.

EGF enhances *MYCN* transcription via recruitment of Sp1 to the *MYCN* promoter

To confirm the EGF-mediated *MYCN* transcription, we generated a luciferase reporter plasmid containing a *MYCN* genomic fragment spanning positions −221 to +21 (Fig. 4A, left panel), where +1 represents the transcriptional initiation site. This promoter region contains both Sp1 and E2F1 transcriptional element sites (31, 32). We also used the empty control vector pGL3basic to compare the EGF responses. SK-N-BE cells were transiently transfected with pGL3basic and pGL3-*MYCN* (−221, +21) together with *Renilla* luciferase reporter plasmid. The data showed that EGF stimulation significantly enhanced the promoter activity of *MYCN* gene at 6 hours (Fig. 4A, right panel): pGL3-Basic reporter constructs did not respond to EGF treatment (Fig. 4A, right), suggesting that EGF treatment is specific to the *MYCN* promoter. *MYCN* has been reported to be transcriptionally regulated by 2 major transcription factors, Sp1 and E2F1 (31, 32). To determine the regulatory mechanism of EGF-mediated *MYCN* transcription, we performed ChIP assays. Both antibodies against Sp1 and E2F1 used for ChIP assays pulled down the specific

Published OnlineFirst July 19, 2012; DOI:10.1158/0008-5472.CAN-12-0943

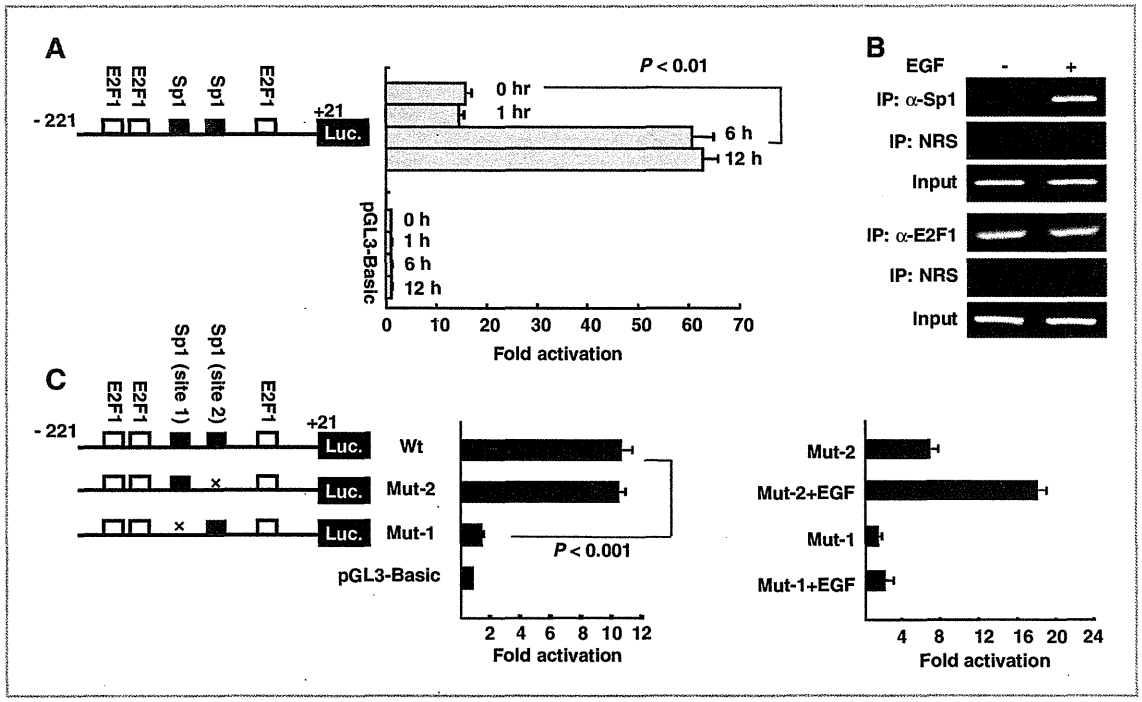

Figure 4. EGF enhances Sp1-mediated transactivation of *MYCN*. A, *MYCN* core promoter region (−221 to +21) cloned in pGL3Basic luciferase vector (left) was transiently transfected into SK-N-BE cells for 36 hours, followed by culture in serum-free medium for 12 hours. Cells were then treated with EGF (50 ng/mL) for the indicated time periods, and luciferase assays were carried out to quantify the relative promoter activity. B, SK-N-BE cells were cultured in serum-free medium for 12 hours, followed by treatment for 12 hours with EGF (50 ng/mL). Cross-linked chromatin was isolated from the cells and precipitated with Sp1- and E2F1-specific antibodies or with normal rabbit serum (NRS). C, Sp1 site 1-deleted *MYCN* core promoter failed to respond to EGF stimulation. Two Sp1-binding sites on the *MYCN* core promoter region were deleted by site-directed mutagenesis (left). Relative activity of the deleted promoter constructs were measured by luciferase assays in SK-N-BE cells 24 hours after transfection (middle). SK-N-BE cells were transiently transfected by the 2 Sp1 site deleted constructs, followed by culture in serum-free medium for 12 hours and then treatment with EGF (50 ng/mL). Twelve hours after EGF treatment, firefly luciferase activities were determined (right). *Renilla* luciferase was used as an internal control to standardize the transfection efficiency of the luciferase vectors.

endogenous proteins (data not shown). Twelve hours after EGF stimulation, chromatin DNA from SK-N-BE cells was cross-linked and processed for ChIP assays. Sp1-derived pulled-down chromatin was amplified by a specific primer targeting the *MYCN* core promoter region (−221 to +21) in the EGF-treated cells (Fig. 4B top panel), suggesting that EGF enhances recruitment of Sp1 to the *MYCN* promoter. However, no change in E2F1 recruitment was observed between the EGF-treated and untreated cells (Fig. 4B, bottom panel).

To identify the critical Sp1-binding region required for the transactivation of *MYCN*, we mutated the Sp1-binding elements (Fig. 4C, left panel) by PCR reactions, as described in the Materials and Methods section. SK-N-BE cells were transiently transfected with wild-type *MYCN* promoter as well as the mutated luciferase constructs. Promoter assays showed that the pGL3MYCN (mut-1) construct had significantly ($P < 0.001$) less promoter activity (Fig. 4C, middle panel) than the wild type and pGL3MYCN (mut-2) constructs. Furthermore, we transiently transfected the wild type, as well as the Sp1 site 1-deleted constructs, into the SK-N-BE cells to determine the effects on EGF. The data showed that the deletion construct failed to respond to EGF treatment (Fig. 4C, right panel), suggesting that the Sp1-binding element 1 is important for EGF-mediated transactivation of *MYCN*.

To check whether Sp1 is critical for the expression of MYCN, we knocked down *Sp1* using siRNAs. Consistently, *MYCN* expression was suppressed in cells transfected with siRNAs against *Sp1* (Supplementary Fig. S2A). Both siRNAs against *Sp1* reduced *MYCN* promoter activity (Supplementary Fig. S2B). Cell proliferation was also suppressed in the *Sp1* knockdown cells (Supplementary Fig. S2C). It has been reported that EGF stimulation induces phosphorylation of ERK, and that this phosphorylation event may be important for Sp1 phosphorylation (33) and recruitment to the target gene promoter. Similarly, our results also showed that EGF treatment resulted in phosphorylation of Sp1, and this phosphorylation event was inhibited in U0126- and calf intestinal phosphatase (CIAP)-treated cells (Supplementary Fig. S3A). CIAP treatment is reported to block recruitment of phosphotranscriptional factors on genomic DNA (35). We also used Mithramycin-A (Mit-A), a well-known Sp1 inhibitor (34). EGF-mediated *MYCN* induction was successfully inhibited in cells pretreated with Mit-A (Supplementary Fig. S3B) and CIAP (Supplementary Fig. S3C). Consistently, CIAP treatment also

Published OnlineFirst July 19, 2012; DOI:10.1158/0008-5472.CAN-12-0943

reduced the recruitment of Sp1 to the *MYCN* promoter (Supplementary Fig. S3D). Collectively, our results suggest that Sp1 recruitment to the *MYCN* promoter can enhance the transactivation of *MYCN* upon EGF treatment.

NLRR1 enhances *MYCN* induction

ERK is reported to induce phosphorylation of Sp1 (33). In our present findings, NLRR1 promotes phosphorylation of ERK upon EGF treatment, suggesting that NLRR1 may induce *MYCN*. Therefore, we overexpressed NLRR1 in SK-N-BE cells and found that endogenous *MYCN* was effectively induced in a dose-dependent manner (Fig. 5A, left panel). NLRR1-mediated *MYCN* induction was inhibited in U0126- and AG1478-pretreated cells (Fig. 5A, right panel), suggesting that NLRR1 induced *MYCN* via EGFR-ERK signaling. Ectopic expression of NLRR1 in cells accelerated *MYCN* induction upon EGF treatment compared with that of mock-transfected (empty pcDNA3.1 vector) cells (Fig. 5B, left panel). Consistent with the overexpression study, knockdown of *NLRR1* suppressed *MYCN* induction, suggesting that NLRR1 accelerates EGF-mediated *MYCN* induction. To determine whether NLRR1 enhances Sp1 recruitment, we performed ChIP assays. The data show that overexpression of NLRR1 in SK-N-BE cells increased Sp1 recruitment to the *MYCN* promoter, which was further accelerated upon EGF treatment (Fig. 5C).

Stable expression of NLRR1 in cells accelerates tumor growth in nude mice

NLRR1 is highly expressed in aggressive *MYCN*-amplified neuroblastoma (14), suggesting the possibility that NLRR1 may have a potent tumorigenic role. NLRR1 overexpression enhanced the colony formation ability of SH-SY5Y cells (Supplementary Fig. S4A). Consistent with our previous observation that ectopic expression of NLRR1 enhanced cell proliferation and inhibited apoptosis, NLRR1-stably expressing SH-SY5Y clones proliferated faster than mock stable clones (Supplementary Fig. S4C). Furthermore, *MYCN* expression was upregulated in NLRR1 stable clones compared with mock clones (Supplementary Fig. S4B), suggesting that NLRR1 has oncogenic potential. To elucidate the tumorigenic activity of NLRR1, we performed tumor xenograft studies in nude mice using NLRR1-stably expressing SH-SY5Y clones. Significant enhancement of tumor growth was observed in mice bearing NLRR1-expressing xenografts compared with the mock-expressing xenografts ($P < 0.01$; Fig. 6A). Mice of each group were sacrificed when they become morbid, and the survival curve was analyzed using the Kaplan–Meier method. The survival of mice with NLRR1-expressing xenografts was significantly shorter compared with mice-bearing mock xenografts ($P = 0.003$; Fig. 6B). Immunohistochemical data showed that NLRR1-expressing tumors had increased numbers of Ki-67–positive cells and decreased number of terminal deoxynucleotidyl transferase–mediated dUTP nick end labeling (TUNEL) positive cells compared with mock tumors (Fig. 6C), indicating that there were more proliferative cells in the tumors derived from NLRR1-expressing clones. To see the consistence *in vitro* finding of NMYC induction by NLRR1, we carried out IHC assays using the tumor xenografts. Induction of NMYC and p-ERK was found in NLRR1 tumors whereas total ERK was unchanged in both tumors (Fig. 6D). Collectively, our data suggest that NLRR1 induces NMYC *in vivo* and has potent tumorigenic roles.

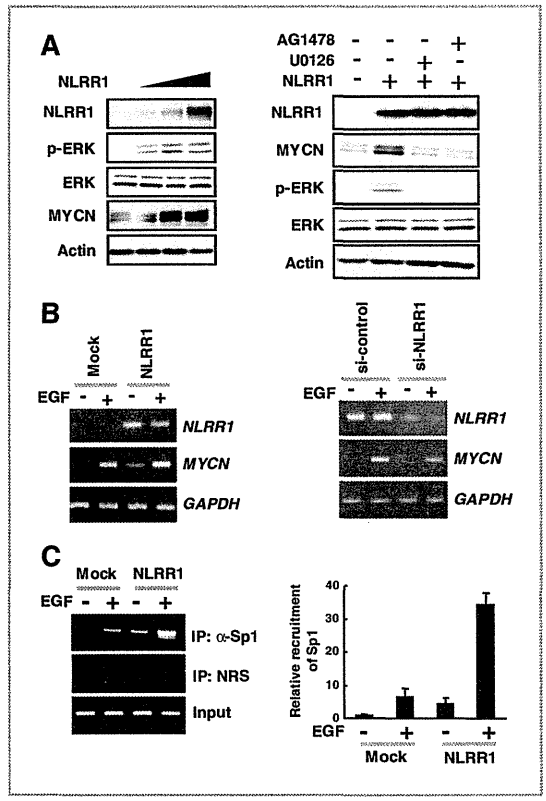

Figure 5. NLRR1 induces MYCN in neuroblastoma cells. A, SK-N-BE cells were transiently transfected with increasing amounts of NLRR1-expressing plasmids. Forty-eight hours after transfection, immunoblotting was carried out to detect NLRR1, p-ERK, total ERK, and MYCN expression (left). EGFR and ERK inhibitors prevent MYCN induction in the NLRR1-overexpressing cells. SK-N-BE cells were transiently transfected with NLRR1 expression plasmids for 48 hours and then treated with or without AG1478 (20 μmol/L) and U0126 (10 μmol/L). Twelve hours after treatment, whole cell lysates were prepared. Immunoblotting data show the expression of NLRR1, p-ERK, total ERK, and MYCN (right). B, NLRR1 enhances *MYCN* induction upon EGF treatment. Twenty-four hours after ectopic expression of NLRR1, SK-N-BE cells were cultured in serum-free medium for 12 hours followed by EGF (10 ng/mL) treatment. RT-PCR was performed to check endogenous *MYCN* expression (left). Forty hours after transfection with control siRNA and NLRR1-siRNA, SK-N-BE cells were serum starved for 12 hours and treated with EGF (10 ng/mL). Twelve hours after EGF treatment, RT-PCR was carried out to check the expression of *NLRR1* and *MYCN* (right). C, crossed-linked chromatin from the SK-N-BE mock- and NLRR1-ectopically expressing cells treated with or without EGF (50 ng/mL) for 12 hours was used for pulldown by Sp1-specific antibody. Primers targeting *MYCN* core promoter (−221, +21) were used to amplify the pulled-down chromatin (left). The recruitment of Sp1 was quantified from the PCR band by image J software and plotted (right). The data represent mean ± SD.